Mon. Not. R. Astron. Soc. **299,** 189–206 (1998)

Depolarization and Faraday effects in galaxies

D. D. Sokoloff,[1⋆] A. A. Bykov,[1⋆] A. Shukurov,[2⋆] E. M. Berkhuijsen,[3⋆] R. Beck[3⋆] and A. D. Poezd[1]

[1]*Physics Department, Moscow University, Moscow 119899, Russia*
[2]*Department of Mathematics, University of Newcastle, Newcastle upon Tyne NE1 7RU*
[3]*Max-Planck-Institut für Radioastronomie, Auf dem Hügel 69, 53121 Bonn, Germany*

Accepted 1998 April 24. Received 1998 April 4; in original form 1997 April 17

ABSTRACT

Faraday rotation and depolarization of synchrotron radio emission are considered in a consistent general approach, under conditions typical of spiral galaxies, i.e. when the magneto-ionic medium and relativistic electrons are non-uniformly distributed in a layer containing both regular and fluctuating components of magnetic field, thermal electron density and synchrotron emissivity. We demonstrate that non-uniformity of the magneto-ionic medium along the line of sight strongly affects the observable polarization patterns. The degree of polarization p and the observed Faraday rotation measure RM are very sensitive to whether or not the source is symmetric along the line of sight. The RM may change sign in a certain wavelength range in an asymmetric slab even when the line-of-sight magnetic field has no reversals. Faraday depolarization in a purely regular magnetic field can be much stronger than suggested by the low observed rotation measures. A twisted regular magnetic field may result in p increasing with λ – a behaviour detected in several galaxies.

We derive expressions for statistical fluctuations in complex polarization and show that random fluctuations in the degree of polarization caused by Faraday dispersion are expected to become significantly larger than the mean value of p at $\lambda \gtrsim 20$–30 cm. We also discuss depolarization arising from a gradient of Faraday rotation measure across the beam, both in the source and in an external Faraday screen. We briefly discuss applications of the above results to radio polarization observations.

We discuss how the degree of polarization is affected by the scaling of synchrotron emissivity ε with the total magnetic field strength B. We derive formulae for the complex polarization at $\lambda \to 0$ under the assumption that $\varepsilon \propto B^2 B_\perp^2$, which may arise under energy equipartition or pressure balance between cosmic rays and magnetic fields. The resulting degree of polarization is systematically larger than for the usually adopted scaling $\varepsilon \propto B_\perp^2$; the difference may reach a factor of 1.5.

Key words: magnetic fields – polarization – radiation mechanisms: non-thermal – galaxies: ISM – galaxies: spiral – radio continuum: general.

1 INTRODUCTION

Basic ideas and results concerning polarization and Faraday rotation in radio sources were discussed by Burn (1966) (see also Korchak & Syrovatskii 1962 and Razin & Khroulyov 1965), who considered such effects as differential Faraday rotation, internal Faraday dispersion and Faraday dispersion in an external screen (see the review of Gardner & Whiteoak 1966). Although unresolved sources were formally considered, many of these results also apply to extended objects. Most interpretations of the radio polarization observations of nearby spiral galaxies are based on the application of Burn's (1966) formulae.

Depolarization and Faraday rotation in synchrotron sources were also discussed by Cioffi & Jones (1980), who considered both resolved and unresolved sources of cylindrical and spherical shape. The role of random magnetic fields was further clarified by Laing (1981), who discussed cylindrical sources (jets) with a partially ordered magnetic field, and Spangler (1982, 1983), who concentrated on correlation properties of well-resolved turbulent fluctuations in a magneto-ionic medium. Statistical properties of

⋆E-mail: sokoloff@lem.srcc.msu.su (DDS); bikov@lem.srcc.msu.su (AAB); Anvar.Shukurov@newcastle.ac.uk (AS); eberkhuijsen@mpifr-bonn.mpg.de (EMB); rbeck@mpifr-bonn.mpg.de (RB)

the random fluctuations in the degree of polarization arising in a random Faraday screen were considered by Tribble (1991). Imprints of magnetohydrodynamic (MHD) turbulence in the observed total and polarized intensity distributions were discussed by Eilek (1989a,b). Depolarization by a finite number of cells with random fields was discussed by Chi, Young & Beck (1997).

The above authors were mainly concerned with applications to radio galaxies, jets and other active radio sources. However, spiral galaxies provide a special environment which deserves a special study. As we show here, the planar stratification typical of flat sources introduces specific features into polarization patterns. Both theory (Sokoloff & Shukurov 1990; Beck et al. 1996) and observations (Berkhuijsen et al. 1997) indicate that the regular magnetic field in galaxies can possess reversals along the line of sight, e.g. between the disc and the halo of a galaxy. The theory must be generalized to include such multi-layer distributions.

It was assumed in earlier papers on polarization in synchrotron sources that the synchrotron emissivity is proportional to the transverse magnetic field squared. Therefore all available results are apparently inapplicable to the case of energy equipartition or pressure balance between magnetic fields and cosmic rays where the scaling with the fourth power of the magnetic field seems to be more appropriate. We discuss the effects of this scaling in Section 5.2.

Radio polarimetric observations of spiral galaxies at decimetre wavelengths and their analyses performed in the recent decade have clearly shown that Faraday depolarization effects are usually strong at these wavelengths (e.g. Sukumar & Allen 1991; Ehle & Beck 1993). On the other hand, polarized emission was detected at wavelengths as long as λ90 cm in the Galaxy (Wieringa et al. 1993) and NGC 891 (De Breuck, de Bruyn & Beck, in preparation). Another unusual property of polarization patterns in spiral galaxies which was discovered only recently is the anomalous depolarization with the degree of polarization increasing with wavelength. This phenomenon was detected in the galaxies M31 (Berkhuijsen, Beck & Gräve 1987), NGC 6946 (Beck 1991) and M51 (Horellou et al. 1992). Similar anomalous depolarization was also detected in the Milky Way long ago (e.g. Bologna, McClain & Sloanaker 1969, their fig. 4), but this went unnoticed.

Strong Faraday rotation of the synchrotron emission from a radio galaxy embedded in a galaxy cluster can arise in the intracluster gas (Dreher, Carilli & Perley 1987; Taylor et al. 1990; Taylor, Barton & Ge 1994; Carilli et al. 1997). Johnson, Leahy & Garrington (1995) pointed out that the observed Faraday depolarization in such a foreground screen does not follow Burn's (1966) result. We discuss Faraday effects in a foreground screen in Sections 7 and 8.2, and in Appendix A.

In this paper we reconsider internal and external depolarization and Faraday rotation effects, especially their aspects that are important for observations of nearby spiral galaxies. We pay special attention to those wavelengths at which most of the observations of galactic magnetic fields have been performed, that is about λλ6 and 20 cm. Some generic configurations of magnetic fields whose ubiquity was understood only recently are included in the analysis. We concentrate mostly on analytically solvable models. Our aim is to develop a general understanding of the effects associated with complicated magnetic configurations in spiral galaxies. Formally, polarization of radio emission is determined by simple integrals that can be easily computed for any specified magnetic field and electron density distribution. Our main concern here is not to describe precisely any specific galaxies, but rather to isolate those parameters of the interstellar medium that affect the polarization pattern substantially. There is hardly any galaxy with parameters that are known in sufficient detail to avoid the use of relatively crude models; our intention is to assess the possible consequences of such a modelling. In particular, we show that polarization patterns are sensitive to whether or not the object is symmetric along the line of sight.

2 THE COMPLEX POLARIZATION

All derivations below start from the following expression for the complex linear polarization of incoherent synchrotron emission (Burn 1966; Gardner & Whiteoak 1966; Pacholczyk 1977):

$$\mathcal{P} = p_{\rm i} \frac{\int_V w(\boldsymbol{r})\varepsilon(\boldsymbol{r}) \exp[2{\rm i}\psi(\boldsymbol{r})]\,{\rm d}V}{\int_V w(\boldsymbol{r})\varepsilon(\boldsymbol{r})\,{\rm d}V}, \qquad (1)$$

$$\psi(\boldsymbol{r}) = \psi_0(\boldsymbol{r}) + K\lambda^2 \int_z^{z_{\rm b}} nB_z\,{\rm d}z.$$

Here $p_{\rm i}$ is the intrinsic degree of polarization, ε is the synchrotron emissivity (i.e. the radiation energy emitted towards the observer per unit time per unit volume in the source); ψ is the local polarization angle at position $\boldsymbol{r}$ (subject to Faraday rotation) and ψ_0 is its intrinsic value (i.e. the intrinsic position of the electric vector of synchrotron emission, which is perpendicular to the local transverse magnetic field $\boldsymbol{B}_\perp$); and λ is the wavelength. $w(\boldsymbol{r})$ is the beam profile, a function of coordinates in the plane of the sky. In most cases we assume $w(\boldsymbol{r}) = 1$ (a flat beam profile), but we consider a Gaussian beam in Section 8. The integrals are taken over the volume V of the beam cylinder in the source of synchrotron emission; z is the coordinate measured along the line of sight with $z = z_{\rm b}$ being the boundary of the object closest to the observer (i.e. the larger of $z_{\rm m}$ and z_ε, the boundaries of the magneto-ionic region and the synchrotron-emitting region, respectively). Further, B_z is the line-of-sight component of the magnetic field; n is the volume density of thermal electrons, and $K = 0.81\,{\rm rad\,m^{-2}\,cm^3\,\mu G^{-1}\,pc^{-1}}$. The intrinsic degree of linear polarization is given by $(3-3\alpha)/(5-3\alpha) \approx 0.75$ with $\alpha \approx -1$ the spectral index of synchrotron emission. Deviations from our assumed value $\alpha \approx -1$ are discussed in Section 5.2.

The real and imaginary parts of $\mathcal{P}$ are observable quantities, the Stokes parameters Q and U normalized by the total synchrotron intensity $I = \int_V \varepsilon\,{\rm d}V$. The modulus of $\mathcal{P}$ is the observed degree of linear polarization, $p = (Q^2 + U^2)^{1/2}/I$, and its argument gives the observed polarization angle, $\Psi = \frac{1}{2}\arctan U/Q$. Hence

$$\mathcal{P} = p\,\exp 2{\rm i}\Psi. \qquad (2)$$

For Faraday-thin objects the observed polarization angle Ψ is a linear function of λ^2, so that the Faraday rotation measure RM can be introduced via $\Psi = \Psi_0 + {\rm RM}\,\lambda^2$. Here Ψ_0 is the observed intrinsic polarization angle at short λ where Faraday rotation is negligible. However, in most cases discussed below Ψ is *not* a linear function of λ^2 (Faraday-thick regimes); in these cases we still formally introduce the Faraday rotation measure as ${\rm RM} = {\rm d}\Psi/{\rm d}(\lambda^2)$, being aware that this is a function of λ. Note that RM obtained from $\Delta\Psi/\Delta(\lambda^2)$ can be quite different from that defined above if $\Delta\lambda \simeq \lambda$ and/or $\Delta\Psi$ is large.

The ratio $p/p_{\rm i}$ is known as depolarization. Those depolarization effects that are related to Faraday rotation lead to a degree of polarization generally decreasing with wavelength (see, however, Section 9). We also discuss in Section 5 depolarization that is independent of Faraday rotation and therefore arises even for $\lambda \to 0$.

We introduce Cartesian coordinates (x, y) in the plane of the sky and the coordinate z measured along the line of sight. The area covered by the telescope beam is denoted W, and the extent of the source along the line of sight is denoted L. Having in mind applications to disc galaxies, it is convenient to fix the origin of the reference frame ($z = 0$) on the symmetry plane if a symmetric source is considered (then $\pm z_\mathrm{b} = \pm\frac{1}{2}L$ are defined as the boundaries of the source) or at the far end of an asymmetric source (then $z_\mathrm{b} = L$). For a distribution of a magneto-ionic medium without a sharp boundary (e.g. exponential or Gaussian distribution), $z_\mathrm{b} = \infty$ can be taken. We neglect the contribution of our Galaxy, the magneto-ionic medium of which acts as a foreground Faraday screen; in most cases of interest, this contribution can be easily allowed for. The total magnetic field vector is denoted $\boldsymbol{B}$; its regular and random components are $\overline{\boldsymbol{B}}$ and $\boldsymbol{b}$, respectively.

3 DIFFERENTIAL FARADAY ROTATION

When synchrotron emission originates in a magneto-ionic medium containing a regular magnetic field, the polarization plane of the radiation produced at different depths within the source is rotated over different angles by the Faraday effect. This results in a decrease in the degree of polarization of the integral emission observed. This effect is known as depolarization by differential Faraday rotation (Gardner & Whiteoak 1966). In this section we consider this effect with allowance for a non-uniform distribution of the magneto-ionic medium in the source. Any variation of parameters perpendicular to the line of sight is neglected in this section (in particular, $w = 1$), and the integrals in equation (1) are taken along the line of sight, z (see Section 8 for a discussion of a gradient of RM across the beam). For moderately inclined galaxies observed with resolutions of 1–3 kpc, this is a very good approximation.

3.1 A uniform slab

Consider a synchrotron-emitting slab with a purely regular magnetic field, $\boldsymbol{B} = \overline{\boldsymbol{B}}$, containing thermal electrons with volume density n. Burn (1966) showed that the complex polarization of intrinsic synchrotron emission of a *uniform* slab is given by

$$\mathcal{P} = p_\mathrm{i}\frac{\sin\mathcal{R}\lambda^2}{\mathcal{R}\lambda^2}\exp 2\mathrm{i}(\psi_0 + \tfrac{1}{2}\mathcal{R}\lambda^2)\,, \qquad (3)$$

where $\mathcal{R} = Kn\overline{B}_z L$ is called here the *intrinsic Faraday rotation measure* (also known as the Faraday depth of the source). Ψ is a linear function of λ^2 and the observable Faraday rotation measure RM is equal to $\frac{1}{2}\mathcal{R}$ in this case.

Equation (3) describes the well-known non-monotonic behaviour of p shown in Fig. 1. Nevertheless, the observational consequences are often confused in the literature. For $\frac{1}{2}\pi < \mathcal{R}\lambda^2 < \pi$, polarized signals from the near and the far side of the slab have rotation angles differing by more than 90° and thus partly cancel, and the observed polarized emission comes from a layer symmetric about the midplane of the slab. Beyond $\mathcal{R}\lambda^2 = \pi$, the first zero-point of p, polarized signals from a large fraction of the slab on the far side, across which the rotation angle is 180°, completely cancel and only polarized emission from a thin layer on the near side is observed. The observable rotation angle caused by the 'visible' layer is only $\frac{1}{2}(\mathcal{R}\lambda^2 - \pi)$.

The observation of Faraday rotation in a wavelength interval including one (or more) wavelengths at which p is zero leads to RM $\neq \frac{1}{2}\mathcal{R}$. However, RM $= \frac{1}{2}\mathcal{R}$ is still valid in wavelength ranges between any two zero-points of p.

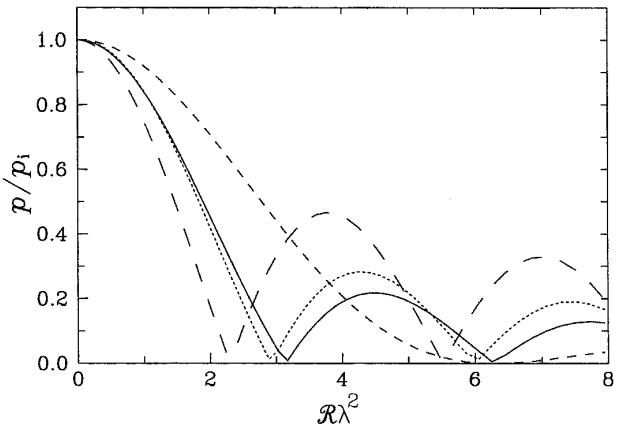

Figure 1. Degree of polarization owing to differential Faraday rotation (i.e. in a purely regular magnetic field) for a symmetric slab with exponential distributions of ε and $n\overline{B}_z$ with $q = h_\mathrm{RM}/h_\varepsilon = 1$ (solid) [this also corresponds to the uniform slab, as described by equation (3)], $q = \frac{1}{2}$ (long dashes), $q = 2$ (short dashes) and $q = (\lambda/10\,\mathrm{cm})^{-0.25}$ (dotted).

Our aim here is to generalize equation (3) in the following two ways: (i) by considering a non-uniform slab, and (ii) by introducing reversals of $\overline{B}_z$ along the line of sight. As we show below, Burn's formula, equation (3), remains applicable if $n\overline{B}_z/\varepsilon =$ constant and $\psi_0 =$ constant along the line of sight.

3.2 A symmetric non-uniform slab

Consider first a slab with arbitrary symmetric distributions of ε, n and $\overline{\boldsymbol{B}}$ along the line of sight, described by $\varepsilon(z) = \varepsilon_0 F(|z|/h_\varepsilon)$ and $n(z)\overline{B}_z(z) = n_0\overline{B}_0 G(|z|/h_\mathrm{RM})$ with the normalization $\int_0^{z_\mathrm{b}} F\,\mathrm{d}z = h_\varepsilon$ and $\int_0^{z_\mathrm{b}} G\,\mathrm{d}z = h_\mathrm{RM}$, where subscript zero denotes the equivalent values and z varies between $-z_\mathrm{b}$ and $+z_\mathrm{b}$. We also assume that ψ_0 is independent of z (then $\psi_0 = \Psi_0$). Then we have from equation (1)

$$p = p_\mathrm{i}\int_0^{z_\mathrm{b}/h_\varepsilon}\mathrm{d}s\,F(s)\cos\left[\mathcal{R}\lambda^2\int_0^{s/q}G(t)\,\mathrm{d}t\right]\,, \qquad (4)$$

$$\Psi = \psi_0 + \tfrac{1}{2}\mathcal{R}\lambda^2\,, \qquad (5)$$

where $\mathcal{R} = K\int_{-z_\mathrm{b}}^{z_\mathrm{b}} n\overline{B}_z\,\mathrm{d}z = Kn_0\overline{B}_0 L$ is the equivalent intrinsic Faraday rotation measure of the slab with $L = 2h_\mathrm{RM}$, $q = h_\mathrm{RM}/h_\varepsilon$, $s = z/h_\varepsilon$ and $t = z/h_\mathrm{RM}$; here $|s| \le z_\mathrm{b}/h_\varepsilon$ and $|t| \le z_\mathrm{b}/h_\mathrm{RM}$. As we can see from equation (5), for any symmetric distribution with $\psi_0 =$ constant we have RM $= \frac{1}{2}\mathcal{R}$ as in the uniform slab, but the degree of polarization (4) differs from that given by equation (3).

Equation (4) reduces to $p = p_\mathrm{i}\sin(\mathcal{R}\lambda^2)/(\mathcal{R}\lambda^2)$ when ε and $n\overline{B}_z$ have similar distributions along the line of sight, i.e. $F = G$, and in addition their scaleheights are identical, i.e. $q = 1$, that is for $n\overline{B}_z/\varepsilon =$ constant. This can be easily seen after integration by parts in equation (4).

We illustrate the behaviour of the degree of polarization using exponential distributions, $F(s) = \exp(-|s|)$ and $G(t) = \exp(-|t|)$ with distinct scaleheights, $q \neq 1$. Other distributions often used in modelling galactic discs are approximations with Gaussian and hyperbolic functions (Spitzer 1942). All these functions give fair fits to the vertical distributions of the gas (Dickey & Lockman 1990) and the synchrotron emission observed in the Milky Way (Beuermann, Kanbach & Berkhuijsen 1985) and edge-on galaxies (Dumke & Krause 1998). We have also tried these approximations, but the differences are insignificant. For the exponential distributions,

equation (4) reduces to

$$p = p_{\rm i} q \int_0^1 s^{q-1} \cos\left[\mathcal{R}\lambda^2(1-s)\right] {\rm d}s \,. \qquad (6)$$

It is easy to find the following approximation:

$$p \approx p_{\rm i}\left[1 - \frac{\mathcal{R}^2\lambda^4}{(q+1)(q+2)}\right] \quad \text{for } \mathcal{R}\lambda^2 \ll 1 \,, \qquad (7)$$

whereas Burn's formula (3) yields $p \approx p_{\rm i}(1 - \frac{1}{6}\mathcal{R}^2\lambda^4)$ in the same limit. In Fig. 1 we show p for different values of q for an exponential symmetric slab as obtained by direct evaluation of the integral in equation (4). In accordance with equation (7), for $q > 1$ (< 1) the degree of polarization for small and moderate values of $\mathcal{R}\lambda^2$ is larger (smaller) than that following from Burn's formula. For $q > 1$, most of the Faraday-rotating medium is located outside the synchrotron layer and does not depolarize, while for $q < 1$ the opposite is true.

Although the qualitative behaviour of p as a function of $\mathcal{R}\lambda^2$ is the same as in a uniform slab, equations (7) and (3) yield the same value of p for values of RM differing by a factor $[6/(q+1)(q+2)]^{1/2}$ (when $\mathcal{R}\lambda^2 \ll 1$). For a typical value of $q = \frac{2}{3}$, which corresponds to $\overline{B} \propto n^{1/2}$ and $\varepsilon \propto \overline{B}^2$, the value of RM corresponding to a given p is then smaller by 25 per cent than that from Burn's formula.

Owing to energy losses of relativistic electrons, h_ε is a function of λ. In the galaxies NGC 891 (Hummel et al. 1991) and M31 (Berkhuijsen, Golla & Beck 1991), the observed behaviour can be approximated as $h_\varepsilon \propto \lambda^{0.25}$. In Fig. 1 we illustrate this case as well. RM is wavelength-independent and equal to $\frac{1}{2}\mathcal{R}$ in the case of constant q, but negligibly varies with λ near this value for the wavelength-dependent q.

3.3 An asymmetric slab

It should be emphasized that the qualitative applicability of the results obtained for a uniform slab, equation (3), to a non-uniform one is connected with the symmetry of the slab with respect to the mid-plane. To illustrate this, we consider an extreme case of asymmetry with $F(s) = \exp(-s)$, $G(t) = \exp(-t)$ and $\psi_0 =$ constant (with $s, t > 0$). Although this can be considered as just one half of the symmetric source discussed in Section 3.2, we show here that the asymmetry results in qualitative changes in the polarization pattern.

For the exponential asymmetric slab, we obtain instead of equation (6)

$$\mathcal{P} = p_{\rm i} \exp(2{\rm i}\psi_0)\, q \int_0^1 s^{q-1} \exp(2{\rm i}\mathcal{R}\lambda^2 s)\, {\rm d}s \,, \qquad (8)$$

where $\mathcal{R} = K n_0 \overline{B}_0 h_{\rm RM}$. Equation (3) is recovered for $q = 1$, so that Burn's formula is also applicable to an asymmetric slab but only when $n\overline{B}_z/\varepsilon =$ constant and $\psi_0 =$ constant.

The integral in equation (8) can be calculated exactly for e.g. $q = 2$, which corresponds to $h_\varepsilon = \frac{1}{2}h_{\rm RM}$:

$$p = p_{\rm i}\frac{1}{S}\left(1 + \frac{\sin^2 S}{S^2} - \frac{\sin 2S}{S}\right)^{1/2},$$

$$\Psi = \psi_0 + \tfrac{1}{2}S + \tfrac{1}{2}\arctan\left(\frac{1}{S} - \frac{1}{\tan S}\right),$$

where $S = \mathcal{R}\lambda^2$. It is obvious that in an asymmetric slab with $q \neq 1$ the polarization angle Ψ is no longer a linear function of λ^2; furthermore, for $q = 2$ we have ${\rm RM} \approx \frac{2}{3}\mathcal{R}$ for $S \ll 1$ and RM approaches $\mathcal{R}$ for $S \gg 1$ instead of ${\rm RM} = \frac{1}{2}\mathcal{R}$ in a uniform slab or for $q = 1$. This occurs because, for $q > 1$, a significant part of the slab acts as a foreground Faraday screen.

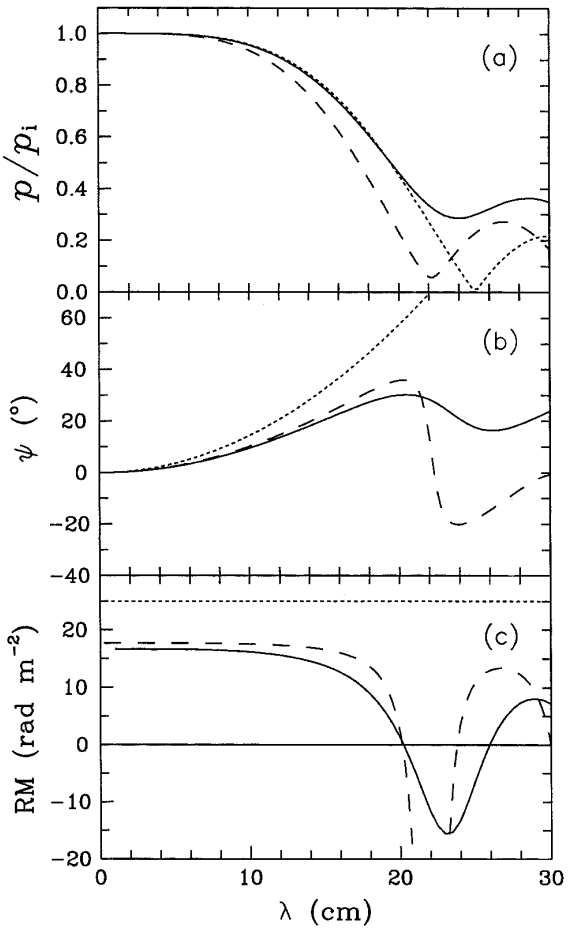

Figure 2. The observable degree of polarization (a), polarization angle (b) and Faraday rotation measure calculated as ${\rm RM} = {\rm d}\Psi/{\rm d}\lambda^2$ (c) in an exponential asymmetric slab with $\mathcal{R} = 50\,{\rm rad\,m^{-2}}$ and $q = h_{\rm RM}/h_\varepsilon = \frac{1}{2}$ (solid), and in a double-layer slab with $\mathcal{R}_1 = 60\,{\rm rad\,m^{-2}}$, $\mathcal{R}_2 = -10\,{\rm rad\,m^{-2}}$ and $I_1/I_2 = 10$ (dashed). The degree of polarization given by equation (3) and the corresponding RM for $\mathcal{R} = 50\,{\rm rad\,m^{-2}}$ are shown dotted.

The degree of polarization, polarization angle and Faraday rotation measure in an asymmetric slab are shown as functions of wavelength in Fig. 2 for $\mathcal{R} = 50\,{\rm rad\,m^{-2}}$ and $q = \frac{1}{2}$, as calculated from equation (8); $q = \frac{1}{2}$ corresponds to $h_\varepsilon = 2h_{\rm RM}$. Note that ${\rm RM} \neq \frac{1}{2}\mathcal{R}$ and RM even changes sign for λ around 20 cm, although the magnetic field has no reversals.

The strong variation and negative values of RM occur at those wavelengths where the deeper part of the slab is (almost) completely depolarized, i.e. $\mathcal{R}\lambda^2 \approx k\pi$, $k = \pm1, \pm2, \ldots$. At shorter wavelengths, the observed polarized emission originates also from the deeper layers, whereas at larger λ an upper layer makes the dominant contribution. This results in strongly varying RM (growing or decreasing with λ in certain wavelength ranges) and even reversed values of RM. This unusual behaviour of RM near $\lambda = 20$ cm may be responsible for singularities in the RM distribution observed in M51 (Horellou et al. 1992).

An RM variation similar to that in Fig. 2 also occurs when differential Faraday rotation is accompanied by Faraday dispersion (see Section 6.2 and Fig. 5, later). However, we stress our result that

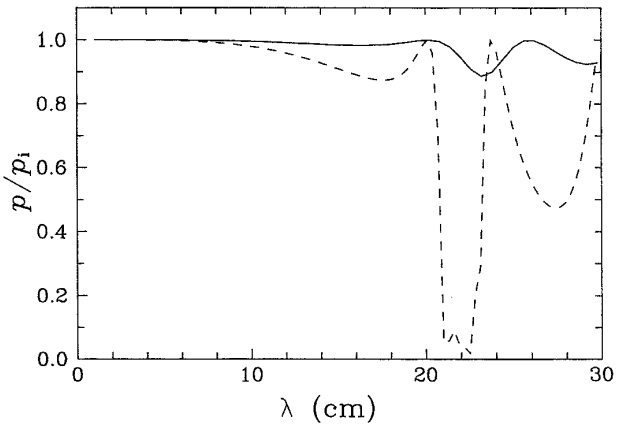

Figure 3. An illustration of the inapplicability of equation (3) to an asymmetric slab and a double-layer distribution of magneto-ionic medium. Shown are the wavelength dependences of the degree of polarization in an exponential asymmetric slab (solid) and a double-layered slab with a reversal in the line-of-sight component of the regular magnetic field (dashed), obtained from Burn's formula, equation (3), with $\mathcal{R}$ replaced by 2 RM, and with the RM shown in Fig. 2(c). The difference from the correct depolarization curves shown in Fig. 2(a) is striking.

RM variations with wavelength may occur already in the case of a *completely regular* field if the slab is asymmetric.

Since RM varies with λ, it is dangerous to apply Burn's formula, equation (3), to an asymmetric slab. To illustrate this, we have used the RM obtained for an exponential asymmetric slab [shown in Fig. 2(c) by a solid line] to calculate the expected degree of polarization from equation (3) by taking $\mathcal{R} = 2$ RM. By comparing the result shown in Fig. 3 with the observable p from Fig. 2(a), we see that the latter is dramatically smaller than that calculated from the observable RM using Burn's formula. It is clear that the reason is that equation (3) is applicable *only* when RM is strictly independent of λ, and application of this equation in more complicated situations can lead to a strong underestimate of the importance of depolarization by differential Faraday rotation.

We conclude that equation (3) is valid for a non-uniform distribution of magneto-ionic medium with a regular magnetic field only when $\psi_0 = \text{constant}$ and $n\overline{B}_z/\varepsilon = \text{constant}$ along the line of sight, or in other words, $n\overline{B}_z$ and ε differ by only a numerical factor independent of z. However, the amount of Faraday rotation expected from the classical Burn formula by inserting the observed values of p can differ strongly from the observable RM values. Deviations from the λ^2 law may indicate a complicated structure of $\overline{B}$ along the line of sight (which makes ψ_0 dependent on z), or an asymmetry in the line-of-sight distribution of the magneto-ionic medium, or a significant contribution of random magnetic fields (see below).

3.4 A multi-layer slab

In this section we discuss differential Faraday rotation in a multi-layer regular magnetic field, including the case of field reversals along the line of sight. This configuration occurs when, for example, the regular magnetic field has different directions in the disc and the halo of a spiral galaxy (Sokoloff & Shukurov 1990; Berkhuijsen et al. 1997), or when a galactic disc hosts a dipole field which may occur in the central parts of galaxies (Donner & Brandenburg 1990; Elstner, Meinel & Beck 1992; Panesar & Nelson 1992), or when the line of sight crosses several spiral arms in a galaxy seen (almost) edge-on.

Consider a slab consisting of N uniform layers with the line-of-sight extent of each layer denoted as L_i, the line-of-sight regular magnetic field as $\overline{B}_i$, the electron density as n_i and the synchrotron intensity originating in the ith layer as I_i. The Nth layer is assumed to be nearest to the observer. It can be shown by direct integration in equation (1) that

$$\mathcal{P} = p_\mathrm{i} \sum_{i=1}^{N} \frac{I_i}{I} \frac{\sin \mathcal{R}_i\lambda^2}{\mathcal{R}_i\lambda^2} \times \exp 2\mathrm{i}\Big(\psi_{0i} + \tfrac{1}{2}\mathcal{R}_i\lambda^2 + \sum_{j=i+1}^{N} \mathcal{R}_j\lambda^2\Big), \quad (9)$$

where $\mathcal{R}_i = Kn_iB_iL_i$ and ψ_{0i} is the intrinsic polarization angle in the ith layer. This expression reduces to equation (3) when all the layers are identical or $N = 1$.

The physical meaning of equation (12) is clear: the emission originating in each layer has the intrinsic degree of polarization depending on $\mathcal{R}_i$ as given by equation (3). When propagating, its polarization angle experiences Faraday rotation with $\mathrm{RM} = \frac{1}{2}\mathcal{R}_i$ in the parent layer and $\mathrm{RM} = \mathcal{R}_j$ in every other layer passed, which then act as a Faraday screen. The total complex polarization is the sum of the complex polarizations arising in each layer weighted with the fractional synchrotron intensity I_i/I (cf. Burch 1979).

Although Faraday rotation in each particular layer follows the λ^2 law, this does not apply to the whole slab, and the resulting degree of polarization is quite different from that given by equation (3). To illustrate this, we give the explicit result for the simplest case of two layers, $N = 2$:

$$p^2 = p_\mathrm{i}^2\left\{A_1^2 + A_2^2 + 2A_1A_2\,\cos^2\left[\Delta\psi_0 + \tfrac{1}{2}(\mathcal{R}_1 + \mathcal{R}_2)\lambda^2\right]\right\}, \quad (10)$$

where $A_i = (I_i/I)\sin(\mathcal{R}_i\lambda^2)/(\mathcal{R}_i\lambda^2)$, $\Delta\psi_0 = \psi_{01} - \psi_{02}$ and the remaining notation is obvious. The polarization angle for an N-layer system is given by

$$\Psi = \tfrac{1}{2}\arctan \frac{\sum_{i=1}^{N} A_i \sin 2[\psi_{0i} + \lambda^2(\frac{1}{2}\mathcal{R}_i + \sum_{j=i+1}^{N}\mathcal{R}_j)]}{\sum_{i=1}^{N} A_i \cos 2[\psi_{0i} + \lambda^2(\frac{1}{2}\mathcal{R}_i + \sum_{j=i+1}^{N}\mathcal{R}_j)]}. \quad (11)$$

This formula can be easily simplified to the case $N = 2$.

Of course, these results agree with those in Sections 3.2 and 3.3 because expressions obtained here can be considered as finite-difference representations of the integrals appearing there. In particular, for any distribution of the layers that is symmetric along the line of sight, i.e. $I_i = I_{N-i}$ and $\mathcal{R}_i = \mathcal{R}_{N-i}$, we have $\mathrm{RM} = \sum_i \frac{1}{2}\mathcal{R}_i$.

3.4.1 *Some applications*

Reversals of magnetic field along the line of sight can strongly affect the observed polarization pattern when the system is asymmetric. However, this can occur even in a symmetric source when the synchrotron emissivity and the magneto-ionic medium have different extents along the line of sight.

To illustrate the above results, consider the galaxy M51, the disc of which is surrounded by an extended magneto-ionic halo and where the synchrotron scaleheight only slightly exceeds the scale-height of the thermal disc (Berkhuijsen et al. 1997). As the far part of the halo does not contribute significantly to the synchrotron emission of the galaxy, only the disc and the near half of the halo

affect the observed polarized radio emission. This introduces an asymmetry along the line of sight.

In Fig. 2 we show the degree of polarization calculated from equation (10), the polarization angle from equation (11), and the Faraday rotation measure for a double-layer slab with $\mathcal{R}_1 = 60\,\mathrm{rad\,m^{-2}}$, $\mathcal{R}_2 = -10\,\mathrm{rad\,m^{-2}}$ and a ratio of synchrotron intensities of $I_1/I_2 = 10$. These values of $\mathcal{R}_1$ and $\mathcal{R}_2$ are close to those obtained by Berkhuijsen et al. (1997) for the disc and halo of M51, respectively. The Faraday rotation measure strongly varies with λ from about $18\,\mathrm{rad\,m^{-2}}$ at small wavelengths to very negative values at $\lambda \approx 23\,\mathrm{cm}$. Negative RM values arise when mainly a layer on the near side of the slab is 'visible' where the field direction is reversed. The RM behaviour looks similar to that of the asymmetric slab (solid lines in Fig. 2) and has a similar explanation (Section 3.3).

In Fig. 3 we show the values of p that would be obtained if equation (3) were applied to a double-layer slab with the values of RM shown dashed in the lower panel of Fig. 2. It is again clear that a direct application of expressions obtained for a case when RM is wavelength-independent (e.g. a uniform slab) with the *observed* values of RM would lead to erroneous results. Faraday depolarization in a purely regular field can be much stronger than the observed low RM suggests. This has to be taken into account in data interpretation.

Another interesting example of a multi-layer magnetic field is a dipole magnetic field which may be maintained by a dynamo in the central part of a spiral galaxy (Donner & Brandenburg 1990; Elstner et al. 1992; Panesar & Nelson 1992). The toroidal and radial components of this field are antisymmetric with respect to the mid-plane, whereas the vertical component is symmetric. When seen at an angle to the symmetry axis, this magnetic configuration is antisymmetric along the line of sight as long as the vertical component can be neglected. Contrary to naive expectations, the total Faraday RM produced by an antisymmetric field does not vanish. Moreover, this configuration produces exactly the same p and RM as just the half of the layer on the near side to the observer. Indeed, for $N = 2$, $I_1 = I_2$ and $\mathcal{R}_1 = -\mathcal{R}_2$, equations (10) and (11) yield $p = p_\mathrm{i}\sin(\mathcal{R}_2\lambda^2)/(\mathcal{R}_2\lambda^2)$ and $\mathrm{RM} = \frac{1}{2}\mathcal{R}_2$. However, this strange degeneracy is removed by internal Faraday dispersion, i.e. by a random magnetic field.

We note that for $N = 2$ and $I_1 = I_2$, the observable rotation measure at small wavelengths becomes

$$\mathrm{RM} \approx \tfrac{1}{4}(\mathcal{R}_1 + 3\mathcal{R}_2) \quad \text{for } \mathcal{R}\lambda^2 \ll \tfrac{1}{2}\pi\,, \tag{12}$$

which also leads to $\mathrm{RM} = \frac{1}{2}\mathcal{R}_2$ for $\mathcal{R}_1 = -\mathcal{R}_2$. This result, showing that the sublayers have different weights, is also far from naive expectations.

3.5 Conclusions of Section 3

A general conclusion of Section 3 is that for a symmetric slab we have $\mathrm{RM} = \frac{1}{2}\mathcal{R}$ in between two consecutive zero-points of p where $\mathcal{R}$ is the total intrinsic Faraday RM of the source (see Section 3.1), but the degree of polarization is different from that given by Burn's formula (3) with the same $\mathcal{R}$. Meanwhile, for an asymmetric slab the degree of polarization is rather close to that given by equation (3), but RM is a function of λ and $\mathrm{RM} \neq \frac{1}{2}\mathcal{R}$ when the scaleheights of ε and $n\overline{B}_z$ differ from each other. When the scaleheights are equal and $\psi_0 = \text{constant}$, equation (3) remains applicable to both symmetric and asymmetric non-uniform slabs.

4 POLARIZATION IN A RANDOM MAGNETIC FIELD: GENERAL CONSIDERATIONS

Consider now the effects associated with the random component of the magnetic field. We assume that the total magnetic field vector $\boldsymbol{B}$ is represented by a regular (large-scale) part $\overline{\boldsymbol{B}}$ and a random one $\boldsymbol{b}$, i.e. $\boldsymbol{B} = \overline{\boldsymbol{B}} + \boldsymbol{b}$. It is assumed that the line-of-sight and transverse components of $\boldsymbol{b}$ are statistically independent to ensure statistical independence of random contributions to ψ_0 and RM. We note that a correlation of $\boldsymbol{b}_\perp$ and b_z can arise owing to the solenoidality of $\boldsymbol{b}$, but we believe that this effect is not important.

Below we use the following notation. The correlation scale of the Faraday rotation measure distribution across the beam is denoted as l_RM and that along the line of sight is l_m. The free-electron density n is a positive random quantity characterized by a correlation scale l_n. Another correlation scale which enters expressions for the complex polarization is l_ε, the correlation scale of the synchrotron emissivity.

It is not easy to express l_m, l_RM and l_ε in terms of the correlation scales of $\boldsymbol{b}$ and n. To illustrate the difficulties, consider the correlation scale of the synchrotron emissivity ε. A widespread model assumes that the fluctuating component of $\boldsymbol{b}$ is a Gaussian random field with a correlation scale d. Then the correlation scale of ε can be understood as, say, the curvature radius of its autocorrelation function at the origin. Then $l_\varepsilon = \frac{1}{2}d$ if $\varepsilon \propto B_\perp^2$.

Another popular model assumes that the magnetic field is regular within each cell of radius d and has independent strengths and orientations in different cells. Then the correlation scale can be introduced in an approximate manner as the scale at which the fields become uncorrelated. It is obvious that $l_\varepsilon = d$ in this case. In a similar model with a spectrum of cell sizes, the correlation scale will depend on the particular way in which space is filled with cells. If the cells are allowed to overlap and the field is assumed to be a vector sum of the fields of the overlapping cells, then the statistical properties of the resulting random field are nearly Gaussian. It is not clear, however, whether or not such a model provides a good description of the interstellar medium.

It is also important to note that n is a positive definite quantity, so that its fluctuations cannot be described as a Gaussian random variable. Therefore reference to Gaussian statistics cannot resolve all problems connected with a statistical description of the magneto-ionic medium. In order to specify relations of l_m, l_RM and l_ε to the correlation scales of $\boldsymbol{b}$ and n, one must develop a detailed statistical model of the random fields involved. The available knowledge is not sufficient for such a model of the interstellar medium.

It is notable that different estimates of the correlation scale of electron density and magnetic fields in the interstellar medium of the Milky Way are in a wide range from a few parsecs to a few hundred parsecs. These values are implied by analyses of Faraday rotation measures of pulsars and extragalactic radio sources (Lazio, Spangler & Cordes 1990; Ohno & Shibata 1993; Minter & Spangler 1996); values around 10 pc follow from the theory of cosmic ray confinement. This range may result from the presence of several physically distinct scales in the distributions of the electron density and/or the magnetic field at which the autocorrelation function has local maxima, or even from the finite size of an observed area. On the other hand, the difference may also arise from the fact that different tracers (the diffusion coefficient of cosmic rays, the observed distribution of RM, scintillations, etc.) have been used to obtain different estimates of the correlation scales. Most plausibly, all these factors contribute and it is difficult to separate them.

Having in mind the above uncertainties, we assume that all the correlation scales l_m, $l_{\rm RM}$ and l_ε are equal to each other in order to obtain expressions for complex polarization which can be used in applications.

Before evaluating the complex polarization in a random field, it is convenient to represent it as follows. Integration over the beam cylinder in equation (1) is equivalent to volume averaging. Since the regular magnetic field as well as the statistical parameters of fluctuations in both $\boldsymbol{B}$ and n can vary along the line of sight, it is expedient to introduce volume averages over a slice of the beam cylinder within which the line-of-sight variation of the averaged parameters can be neglected. The extent of this slice along the line of sight should be significantly smaller than the scaleheights of the constituents of the magneto-ionic medium.

Having identified volume integrals with the corresponding averages, equation (1) can be rewritten as

$$\mathcal{P} = p_{\rm i} \frac{\int_V \mathrm{d}V \left\langle \varepsilon \exp 2\mathrm{i}\psi_0 \right\rangle_{W\times h} \left\langle \exp 2\mathrm{i}K\lambda^2 \int_z^{z_{\rm b}} nB_z \,\mathrm{d}z' \right\rangle_{W\times h}}{\int_V \mathrm{d}V \langle \varepsilon \rangle_{W\times h}} ,$$

where $\langle \ldots \rangle_{W\times h}$ denotes averaging over the slice volume $W \times h$ in the synchrotron source; these averages are slowly varying functions of position. It is convenient to represent the latter expression in the following equivalent form:

$$\mathcal{P} = \frac{\int_V \mathrm{d}V \, \mathcal{P}_0 \langle \varepsilon \rangle_{W\times h} \left\langle \exp 2\mathrm{i}K\lambda^2 \int_z^{z_{\rm b}} nB_z \,\mathrm{d}z' \right\rangle_{W\times h}}{\int_V \mathrm{d}V \langle \varepsilon \rangle_{W\times h}} , \tag{13}$$

where

$$\mathcal{P}_0 = p_{\rm i} \frac{\left\langle \varepsilon \exp 2\mathrm{i}\psi_0 \right\rangle_{W\times h}}{\langle \varepsilon \rangle_{W\times h}} \tag{14}$$

is the complex intrinsic polarization averaged over the random fluctuations.

Thus the assumption that $\boldsymbol{b}_\perp$ and b_z are uncorrelated allows us to factorize the integrand in equation (1) to obtain equation (13), i.e. to decouple the effects of the wavelength-independent depolarization represented by $\mathcal{P}_0$ and Faraday effects described by the exponential term in (13). In the following sections we discuss these two groups of effects separately, and then consider examples of their combined action.

5 WAVELENGTH-INDEPENDENT DEPOLARIZATION

In this section we evaluate $\mathcal{P}_0$, the complex polarization at $\lambda \to 0$. Depolarization at short wavelengths is due to mixing of emission with different polarization planes within the telescope beam. This depolarization is wavelength-independent; it can be observed at small wavelengths where Faraday effects are negligible.

The problem reduces to the calculation of the volume averages in equation (14). Let us assume that the volume of a slice encompasses a large number of correlation cells. Using the ergodic hypothesis, a volume average can be expressed in terms of the ensemble average as the sum of a regular and a fluctuating part:

$$\langle X \rangle_{W\times h} \approx \langle X \rangle + N_W^{-1/2} \sigma_X \xi ,$$

where X is a complex random variable (not necessarily a Gaussian one), $\langle \ldots \rangle$ denotes the ensemble average, N_W is the number of correlation cells of X within the averaging volume of a slice, σ_X is the standard deviation of X defined as $\sigma_X^2 = \langle XX^* \rangle - \langle X \rangle \langle X^* \rangle$, with the asterisk denoting the complex conjugate, and ξ is a complex random variable with zero mean value and unit standard deviation. Direct application of this formula to equation (14) yields

$$\mathcal{P}_0 = p_{\rm i} \frac{\left\langle \varepsilon \exp 2\mathrm{i}\psi_0 \right\rangle + N_W^{-1/2} \sigma_0 \xi_1}{\langle \varepsilon \rangle + N_W^{-1/2} \sigma_\varepsilon \xi_2} , \tag{15}$$

where σ_0 and σ_ε are the standard deviations of $\varepsilon \exp(2\mathrm{i}\psi_0)$ and ε, respectively, and ξ_1 and ξ_2 are complex and real random variables, respectively, both with zero mean and unit variance. Here we have assumed for simplicity that both $\varepsilon \exp(2\mathrm{i}\psi_0)$ and ε have N_W correlation cells in the beam area.

To evaluate the averages in equation (19) we note that $\langle B_i \rangle = \overline{B}_i$ and $\langle B_i^2 \rangle = \overline{B}_i^2 + \sigma_i^2$, where σ_i is the standard deviation of b_i. We also introduce Cartesian coordinates in the plane of the sky (x, y) with the corresponding axes oriented along the principal axes of the covariance matrix of the random field $\boldsymbol{b}_\perp$; this ensures that $\langle b_x b_y \rangle = 0$. $\boldsymbol{b}$ can be an anisotropic random vector, $\sigma_x \neq \sigma_y \neq \sigma_z$.

5.1 Generalization of the standard approach

As the intrinsic polarization plane is perpendicular to $\boldsymbol{B}_\perp$, we have

$$\psi_0 = \tfrac{1}{2}\pi + \arctan B_y/B_x . \tag{16}$$

Assuming a synchrotron spectral index of $\alpha = -1$, so that

$$\varepsilon = cB_\perp^2 \tag{17}$$

with a certain constant c depending on the number density of relativistic electrons, this yields

$$\varepsilon \exp(2\mathrm{i}\psi_0) = c(B_x^2 - B_y^2 + 2\mathrm{i}B_x B_y) .$$

As we discuss in Section 5.2, the error associated with the approximation $\alpha = -1$ is smaller than other uncertainties of the modelling.

After some simple algebra, equation (19) reduces to the sum of the regular and fluctuating parts of the form

$$\mathcal{P}_0 \approx p_0 \exp(2\mathrm{i}\Psi_0) + N_W^{-1/2} \sigma_* \xi_* , \tag{18}$$

where

$$p_0 = p_{\rm i} \frac{\left[\left(\overline{B}_x^2 - \overline{B}_y^2 + \sigma_x^2 - \sigma_y^2 \right)^2 + 4\overline{B}_x^2 \overline{B}_y^2 \right]^{1/2}}{\overline{B_\perp^2}} , \tag{19}$$

$$\Psi_0 = \tfrac{1}{2}\pi + \tfrac{1}{2} \arctan \left(\frac{2\overline{B}_x \overline{B}_y}{\overline{B}_x^2 - \overline{B}_y^2 + \sigma_x^2 - \sigma_y^2} \right) , \tag{20}$$

$$\sigma_* \xi_* = \left(\sigma_0 / \overline{B_\perp^2} \right) \xi_1 - \left(p_0 \sigma_\varepsilon / \overline{B_\perp^2} \right) \xi_2 , \tag{21}$$

where $\overline{B}_\perp^2 = \overline{B}_x^2 + \overline{B}_y^2$, $\overline{B_\perp^2} = \overline{B}_\perp^2 + \sigma_x^2 + \sigma_y^2$, and the overbar denotes ensemble averaging (equivalent to $\langle \ldots \rangle$); we note that ξ_1 and ξ_2 are not statistically independent and $N_W \gg 1$ is assumed. We stress again that p_0, Ψ_0 and σ_* can be functions of z.

The following expressions for σ_0 and σ_ε in equation (21) can be obtained by direct calculations from $\sigma_X^2 = \langle XX^* \rangle - \langle X \rangle \langle X^* \rangle$, assuming that $\boldsymbol{b}_\perp$ is an isotropic Gaussian random variable, so that $\langle b_i^4 \rangle = 3\sigma^4$:

$$\sigma_0^2 = 8\sigma^2(\overline{B}_\perp^2 + \sigma^2) , \qquad \sigma_\varepsilon = 4\sigma^2(\overline{B}_\perp^2 + 2\sigma^2) ,$$

where $\sigma = \sigma_x = \sigma_y = \sigma_z$.

Equation (18) expresses an intuitively obvious fact that both the degree of polarization and the polarization angle arising in a

random field have predictable values only provided that the number of correlation cells is large enough, so that the first term in equation (18) dominates. Otherwise, the complex polarization is simply a random vector.

It is useful to obtain limitations on the number of correlation cells within the beam cylinder required to have sufficiently small random fluctuations in the observable polarization. After integration over z in equation (13), N_W should be replaced by N, the number of correlation cells within the beam cylinder, i.e. a region of area W and depth L. From equations (18) and (21) we have that the regular term is larger than that arising from the fluctuations, provided that $N^{1/2} \gtrsim \sigma_0 (p_0 \overline{B_\perp^2})^{-1}$ and $N^{1/2} \gtrsim \sigma_\varepsilon / \overline{B_\perp^2}$. For an isotropic Gaussian random magnetic field, the first inequality reduces to

$$N \gtrsim 8 \left(\frac{\sigma}{\overline{B}_\perp}\right)^2 \left[1 + \left(\frac{\sigma}{\overline{B}_\perp}\right)^2\right], \tag{22}$$

where N is the number of correlation cells of $\varepsilon \exp(2\mathrm{i}\psi_0)$ within the beam cylinder $W \times L$. This yields $N \gtrsim 100$ for a typical case of $\left(\sigma/\overline{B}_\perp\right)^2 = 3$. The second inequality for $N^{1/2}$ above leads in this case to a much less stringent constraint $N \gtrsim 2$.

We give an explicit expression for N which should be used to isolate, using equation (26), the cases when neglect of the second term in equation (18) is meaningful:

$$N = \begin{cases} L/(2l) & \text{for } D \lesssim 2l, L \gg 2l\,, \\ LD^2/(2l)^3 & \text{for } D \gg 2l, L \gg 2l\,, \\ D^2/(2l)^2 & \text{for } D \gg 2l, L \lesssim 2l\,, \end{cases} \tag{23}$$

where D is the beam diameter and l is the correlation scale. We recall that correlation scales of all fluctuating quantities are supposed to be equal to each other. The first case corresponds to a very narrow beam and a thick slab, the second to a wide beam and a thick slab, and the third to a thin slab observed at low resolution. The case of a narrow beam and thin slab, $D \ll 2l$ and $L \ll 2l$, is trivial because then the medium cannot be considered random.

In an intermediate case when the fluctuations are partially resolved and the number of correlation cells within the volume $W \times L$ is only moderate, that is $D \simeq 2l$ and $L \simeq 2l$, equation (18) remains applicable with the regular magnetic field understood as being the mean over the beam cylinder. Then the resulting polarization angle becomes random. The variance of the random magnetic field σ^2 becomes a function of the beam size D and should be replaced by $A(D)$, where $A(\delta r) = \langle \boldsymbol{b}(\boldsymbol{\delta r}) \cdot \boldsymbol{b}(\boldsymbol{r} + \boldsymbol{\delta r}) \rangle$ is the autocorrelation function.

5.1.1 *Some applications*

If all relevant quantities entering equations (18)–(21) are independent of z and $\lambda \to 0$ or $n = 0$, integration over z in equation (13) becomes trivial. Then we obtain the following two well-known examples of wavelength-independent polarization as particular cases of equations (19) and (20).

In an isotropic random field, $\sigma_x = \sigma_y = \sigma$, superimposed on a regular magnetic field $\overline{B}$, the ensemble-averaged complex polarization becomes (Korchak & Syrovatskii 1962; Burn 1966)

$$\left\langle \mathcal{P}_0 \right\rangle = p_\mathrm{i} \frac{\overline{B}_\perp^2}{\overline{B}_\perp^2 + 2\sigma^2} \exp 2\mathrm{i}\left[\tfrac{1}{2}\pi + \arctan\left(\overline{B}_y / \overline{B}_x\right)\right], \tag{24}$$

where we recall that σ is the *one-dimensional* standard deviation of the random magnetic field; so $2^{1/2}\sigma$ is the rms value of $\boldsymbol{b}_\perp$.

Another interesting example is a purely random anisotropic magnetic field, $\overline{\boldsymbol{B}}_\perp = 0$, $\sigma_x \neq \sigma_y$, and $\overline{B_\perp^2} = \sigma_x^2 + \sigma_y^2 \neq 0$. Such a magnetic field also produces polarized emission, the complex polarization of which follows from equations (19) and (20) as

$$\left\langle \mathcal{P}_0 \right\rangle = p_\mathrm{i} \frac{\sigma_x^2 - \sigma_y^2}{\sigma_x^2 + \sigma_y^2} \exp \mathrm{i}\pi\,. \tag{25}$$

The resulting polarization angle is $\Psi_0 = \frac{1}{2}\pi$ as measured from the x-axis, which is chosen to be parallel to the direction along which the standard deviation of $\boldsymbol{b}_\perp$ is a maximum. A two-dimensional random, isotropic magnetic field confined to a plane that is inclined by an angle β to the line of sight (Laing 1981) is a particular case of this configuration; Laing's result (1981, his section 3) is recovered from equation (29) when $\sigma_y = \sigma_x \sin\beta$.

We note that the above results do *not* rely on the Gaussian statistical properties of the fluctuations.

Polarization associated with anisotropy in $\boldsymbol{b}$ can be significant in galaxies. A polarization degree of 10 per cent is produced in quite a weakly anisotropic magnetic field with $\sigma_x/\sigma_y = 1.14$. Such an anisotropy can readily arise in the discs of spiral galaxies owing to azimuthal stretching of turbulent cells by differential rotation, and in galactic haloes owing to vertical stretching by galactic fountains and/or winds. This can mimic a regular magnetic field – azimuthal in the disc and vertical in the halo. However, RM must be small in both isotropic and anisotropic random magnetic fields. A significant Faraday RM is a signature of a regular magnetic field.

To illustrate the use of equation (18), consider a spiral galaxy. A typical size of a turbulent cell is then $2l = 10$–100 pc in the disc and $2l = 100$–1000 pc in the halo (see Sokoloff & Shukurov 1990; Poezd, Shukurov & Sokoloff 1993; Dumke et al. 1995). The characteristic line-of-sight depth of the magneto-ionic medium is $L = 2$ kpc in the disc seen nearly face-on and $L = 10$ kpc in the halo of a galaxy seen nearly edge-on. For a beam diameter $D = 0.5$ kpc we have $D \gg 2l$ and $L \gg 2l$ in the disc and $D \simeq 2l$ and $L \gg 2l$ in the halo. Thus $N_\mathrm{disc} \simeq LD^2/(2l)^3 \simeq 5 \times (10^2$–$10^5)$ and $N_\mathrm{halo} \simeq L/(2l) \simeq 20$–$100$. Comparing this with equation (26) for $\sigma^2/\overline{B}_\perp^2 = 3$, we see that the regular part of $\mathcal{P}_0$ significantly exceeds (by modulus) the fluctuations in the disc, but in the halo of a galaxy seen edge-on the fluctuations are comparable to the mean value of $\mathcal{P}_0$. Thus wavelength-independent depolarization would make observations of the polarization of the intrinsic synchrotron emission from galactic haloes at this high resolution meaningless, and the data must be smoothed to a *coarser* resolution in order to yield any useful estimates of the physical parameters (a correlation analysis of fluctuations in the polarization pattern is the only reasonable approach in the case of such high-resolution observations). For moderately inclined galaxies, the strong difference between the synchrotron emissivities in the disc and the halo makes the fluctuations in $\mathcal{P}_0$ arising in the halo less important.

5.2 Energy equipartition between magnetic fields and cosmic rays

All available analyses of the polarization of synchrotron sources assume that the synchrotron emissivity scales as $\varepsilon \propto B_\perp^2$. This assumption also was adopted in our discussion above. However, the scaling of synchrotron emissivity with magnetic field is different under the widely used assumptions of energy equipartition and pressure equilibrium between magnetic fields and cosmic rays. In this case the number density of energetic particles scales as B^2 if the energy densities of magnetic fields and cosmic rays are completely correlated, and the scaling becomes

$$\varepsilon = CB^2 B_\perp^2 \tag{26}$$

with a certain constant C. The stronger dependence of the synchrotron emissivity on magnetic field increases the importance of regions with strong B (both localized and extended). Therefore, the degree of polarization under the scaling (26) must be generally larger than that of (17). This affects both p at $\lambda \rightarrow 0$ and the Faraday effects in any inhomogeneous regular and/or random magnetic field.

For illustration we derive here an expression for the complex polarization at short wavelengths for the scaling (26). In this case

$$\varepsilon \exp(2\mathrm{i}\psi_0) = CB^2(B_x^2 - B_y^2 + 2\mathrm{i}B_xB_y) ,$$

which yields

$$p = p_\mathrm{i}\left(\overline{B^2}\,\overline{B_\perp^2}\right)^{-1} \times \left\{\left[\overline{B}_x^4 - \overline{B}_y^4 + 3\left(\sigma_x^4 - \sigma_y^4\right) + 6\left(\overline{B}_x^2\sigma_x^2 - \overline{B}_y^2\sigma_y^2\right) + \overline{B_z^2}\left(\overline{B_x^2} - \overline{B_y^2}\right)\right]^2 + 4\overline{B}_x^2\overline{B}_y^2\left[\overline{B^2} + 2\left(\sigma_x^2 + \sigma_y^2\right)\right]^2\right\}^{1/2},$$

where the same notation as in Section 5.1 is used and ψ_0 is given by equation (20). It is instructive to consider a purely transverse field consisting of a uniform component and an isotropic random field with $\sigma_x = \sigma_y \equiv \sigma$, $\overline{B}_z = \sigma_z = 0$ and $\overline{B}_\perp = \overline{B}_x$. Then

$$p = p_\mathrm{i}\frac{1 + 6\left(\sigma/\overline{B}_\perp\right)^2}{1 + 8\left(\sigma/\overline{B}_\perp\right)^2 + 8\left(\sigma/\overline{B}_\perp\right)^4} , \qquad (27)$$

which should be compared with equation (24). As we can see, the scalings (17) and (26) lead to very similar degrees of polarization for $\sigma/\overline{B}_\perp \ll 1$, but p is larger by 50 per cent under the assumption of energy equipartition and for $\sigma/\overline{B}_\perp \gg 1$.

The synchrotron emissivity (26) and, consequently, p depend on the line-of-sight magnetic field via the energy density of relativistic electrons. For an isotropic random field, $\sigma_x = \sigma_y = \sigma_z \equiv \sigma$, and a vanishing line-of-sight component of the regular field, $\overline{B}_z = 0$ and $\overline{B}_\perp = \overline{B}_x$, we obtain

$$p = p_\mathrm{i}\frac{1 + 7\left(\sigma/\overline{B}_\perp\right)^2}{1 + 9\left(\sigma/\overline{B}_\perp\right)^2 + 10\left(\sigma/\overline{B}_\perp\right)^4} . \qquad (28)$$

In the limiting case $\sigma/\overline{B}_\perp \gg 1$, equation (28) yields $p/p_\mathrm{i} \simeq 1.4\overline{B}_\perp^2/b_\perp^2$ (with $b_\perp^2 = 2\sigma^2$), which is larger by 40 per cent than equation (24) gives, but the asymptotic dependence of p on $\sigma/\overline{B}_\perp$ remains the same as in equation (24).

In Fig. 4 we illustrate the effect of the scaling (26) on the degree of polarization in a uniform slab with a partially ordered magnetic field with $\overline{B}_z = 0$, $\sigma = 1.6\overline{B}_\perp$, where σ is the one-dimensional standard deviation of the isotropic random magnetic field, and $\sigma_\mathrm{RM}^2 = 1900\,\mathrm{rad^2\,m^{-4}}$. The intrinsic degrees of polarization obtained under the scalings (17) and (26) differ by as much as 25 per cent at $\lambda \rightarrow 0$. We also include the internal Faraday dispersion discussed in Section 6 which is affected by the scaling of the synchrotron emissivity with magnetic field as well.

The results of this section allow us to assess the role of the deviations of the synchrotron spectral index α from the assumed value of -1. The dependence $\varepsilon \propto B_\perp^4$, close to what was discussed above, would correspond, without any equipartition, to an extremely steep spectrum with $\alpha = -3$. As shown in Fig. 4, even a strong change of α from -1 to -3 results in a moderate variation in p of just 20–30 per cent. The observed variations of α for optically thin objects (like discs and haloes of galaxies), $-1.1 \lesssim \alpha \lesssim -0.8$, therefore produce relatively unimportant variations in the polarization pattern.

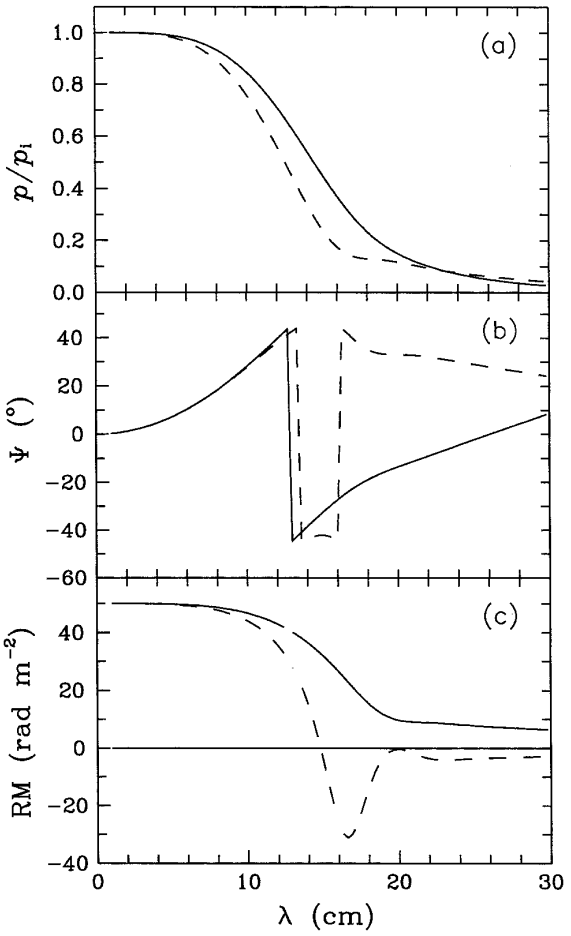

Figure 4. In the case of energy equipartition between magnetic fields and cosmic rays, $\varepsilon \propto B^2B_\perp^2$, the polarization in a partially ordered magnetic field (solid) is stronger than for $\varepsilon \propto B_\perp^2$ (dashed). Shown is the case of a transverse regular magnetic field $\overline{B}_\perp = 5\,\mu\mathrm{G}$ and an isotropic random field with $\sigma = 1.6\overline{B}_\perp = 8\,\mu\mathrm{G}$, and $\sigma_\mathrm{RM}^2 = 1900\,\mathrm{rad^2\,m^{-4}}$. The random field is uniform within the cells of size $l = 50\,\mathrm{pc}$. The degree of polarization at $\lambda \rightarrow 0$ is given by equation (28); the random field causes internal Faraday dispersion at $\lambda \neq 0$.

6 INTERNAL FARADAY DISPERSION

6.1 General considerations

The polarization plane of emission propagating in a random magneto-ionic medium experiences a random walk which causes depolarization when the telescope beam encompasses many turbulent cells. These lead to different amounts of Faraday rotation along different lines of sight within the beam. If this effect occurs within a synchrotron-emitting region it is called internal Faraday dispersion and is described by the wavelength-dependent term in equation (13), which is the subject of this section.

We introduce regular and random components, M and m, of the product

$$KnB_z = M + m \qquad (29)$$

which includes the density of thermal electrons as well as magnetic fields. As shown in Appendix A, the complex polarization is then

given by

$$\mathcal{P} = \left(\int_{-z_b}^{z_b} \langle\varepsilon\rangle_{W\times h}\,\mathrm{d}z\right)^{-1} \times \int_{-z_b}^{z_b} \mathcal{P}_0\Big\{\langle\varepsilon\rangle \exp\big[\textstyle\int_z^{z_b}(2\mathrm{i}\lambda^2 M - 2\lambda^4\sigma_m^2 l_m)\,\mathrm{d}z'\big] + N_W^{-1/2}\Xi\Big\}\,\mathrm{d}z\,, \tag{30}$$

where l_m and σ_m are the correlation scale along z and the standard deviation of m, respectively. N_W is the number of correlation cells in the beam area. $\mathcal{P}_0$, possibly a function of z, was evaluated in Section 5 and Ξ, a complex random quantity the dispersion of which is calculated in Appendix A, represents fluctuations.

6.2 Internal Faraday dispersion in a symmetric slab

Consider a slab with $\langle\varepsilon\rangle$, M and σ_m^2 being symmetric functions of z, i.e. $\langle\varepsilon\rangle = \varepsilon_0 F(|z|/h_\varepsilon)$, $M = (2h_M)^{-1}\mathcal{R} f(|z|/h_M)$ and $\sigma_m^2 = (2h_m)^{-1}\sigma_{\rm RM}^2\, g(|z|/h_m)$, where

$$\mathcal{R} = 2M_0 h_M \quad \text{and} \quad \sigma_{\rm RM}^2 = 2\sigma_{m0}^2 l_m h_m\,; \tag{31}$$

h_M has the same physical meaning as $h_{\rm RM}$ used in Section 3 where a purely regular magnetic field was considered; σ_{m0} is σ_m at $z = 0$. (Note that h_m is defined as the scaleheight of σ_m^2 rather than of σ_m.)

Apart from σ_m, defined as the standard deviation of m (the fluctuating part of KnB_z), below we also use the standard deviation of the integral $\int_{-z_b}^{z_b} m\,\mathrm{d}z'$, which is denoted as $\sigma_{\rm RM}$.

Adopting the normalization $\int_0^{z_b} F(z/h_\varepsilon)\,dz = h_\varepsilon$, $\int_0^{z_b} f(z/h_M)\,\mathrm{d}z = h_M$ and $\int_0^{z_b} g(z/h_m)\,\mathrm{d}z = h_m$, the quantities with subscript zero in equation (31) are equivalent values.

If $\langle\mathcal{P}_0\rangle$ is independent of z, the ensemble average of the complex polarization given by equation (30) reduces to

$$\langle\mathcal{P}\rangle = \tfrac{1}{2}\langle\mathcal{P}_0\rangle \int_{-z_b/h_\varepsilon}^{z_b/h_\varepsilon} \mathrm{d}s\, F(|s|) \times \exp \int_{s/q}^{z_b/h_M} \mathrm{d}t\,[\mathrm{i}\lambda^2\mathcal{R} f(|t|) - \lambda^4\sigma_{\rm RM}^2 q_m g(q_m|t|)], \tag{32}$$

where $q = h_M/h_\varepsilon$, $q_m = h_M/h_m$ and the integration variables are $s = z/h_\varepsilon$ and $t = z'/h_M$. This expression can be further simplified to

$$\langle\mathcal{P}\rangle = \langle\mathcal{P}_0\rangle \exp(-\lambda^4\sigma_{\rm RM}^2 + \mathrm{i}\lambda^2\mathcal{R}) \int_0^{z_b/h_\varepsilon} \mathrm{d}s\, F(s) \times \cosh \int_0^{s/q} \mathrm{d}t\,[\lambda^4\sigma_{\rm RM}^2 q_m g(q_m t) - \mathrm{i}\lambda^2\mathcal{R} f(t)]\,. \tag{33}$$

For $q = q_m = 1$ and $F = f = g$ (i.e. for identical distributions of all the constituents of the magneto-ionic medium along the line of sight), integration in equation (33) can be performed exactly to yield

$$\langle\mathcal{P}\rangle = \langle\mathcal{P}_0\rangle \frac{1 - \exp(-S)}{S}\,, \tag{34}$$

where $S = 2\lambda^4\sigma_{\rm RM}^2 - 2\mathrm{i}\lambda^2\mathcal{R}$ and $\sigma_{\rm RM}$ and $\mathcal{R}$ are defined in equation (31). Equation (34) coincides with the well-known result of Burn (1966) who obtained it for a particular case of a uniform slab (note a factor of 2 in the first term of S which was missed by Burn).

We illustrate the effects of internal Faraday dispersion in Fig. 5. It seems to be realistic to adopt $\langle\varepsilon\rangle_{W\times h} \propto M^2$ and $\sigma_m \propto M$, i.e. $q = q_m = 2$, which applies where the synchrotron emissivity scales as magnetic field squared and regular and random magnetic fields have equal scaleheights. Solid lines show results obtained in this case from equation (33) for a symmetric Gaussian slab with $f(t) = (2/\pi)^{1/2}\exp(-\frac{1}{2}t^2)$. This yields a sign-constant RM. For comparison, results for the same $f(t)$ and h_M but with $\langle\varepsilon\rangle \propto M$ and $\sigma_m^2 \propto M$, i.e. $q = q_m = 1$, when equation (34) applies, are shown dashed (we note that this scaling does not seem to be realistic). The values of parameters chosen are $\mathcal{R} = 100\,\mathrm{rad\,m^{-2}}$ and $\sigma_{\rm RM}^2 = 1000\,\mathrm{rad^2\,m^{-4}}$, which corresponds to values $n = 0.03\,\mathrm{cm^{-3}}$, $\overline{B}_z = 2\,\mu\mathrm{G}$, $\sigma_z = 3\,\mu\mathrm{G}$, $l_m = 100\,\mathrm{pc}$ and $h_\varepsilon = 1\,\mathrm{kpc}$, typical for the discs of spiral galaxies. The results for an exponential slab with the same equivalent parameters are practically the same.

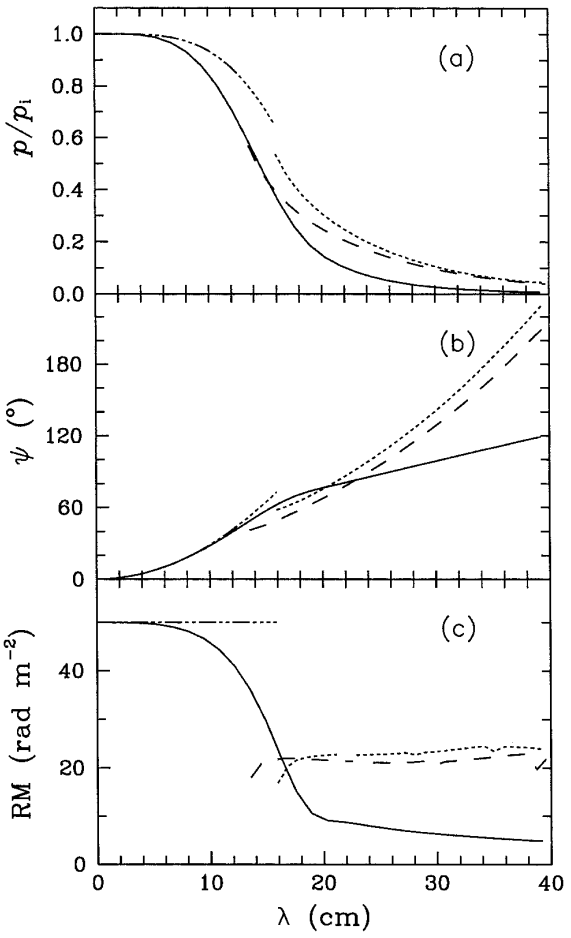

Figure 5. Internal Faraday dispersion in a symmetric Gaussian slab containing both regular and random magnetic fields with scaleheights $h_\varepsilon = h_m = \frac{1}{2}h_M$ (solid), and for $h_\varepsilon = h_m = h_M$ (dashed). The latter results are the same as for a uniform slab. (a) The degree of polarization; (b) the polarization angle; and (c) the corresponding values of $\mathrm{RM} = \mathrm{d}\Psi/\mathrm{d}(\lambda^2)$. Note a change of the sign of RM appearing for a uniform slab and for $h_\varepsilon = h_m = h_M$, although $\overline{B}_z$ is sign-constant. This does not occur for a more realistic model shown with solid lines.

Fig. 5 shows that, unlike the case of differential Faraday rotation in a regular magnetic field (Fig. 1), the degree of polarization in a random magnetic field is not very sensitive to the relation between the scaleheights, so that Burn's formula equation (34) well approximates p in a non-uniform slab. However, RM exhibits a significant dependence on the distribution of the magneto-ionic medium along the line of sight. RM remains positive at all wavelengths when the ratio of the random and regular magnetic fields is independent of z (i.e. $h_m = \frac{1}{2}h_M$) and the synchrotron emissivity has the same scaleheight as m. A general feature of Faraday rotation is that

equation (34), applicable to a uniform slab and to the case $h_\varepsilon = h_m = h_M$, yields reversed values of RM in a certain range of λ even when the regular magnetic field has no reversals along the line of sight. A similar result was obtained by Chi et al. (1997) based on a somewhat simpler model of mixed regular and random fields.

6.3 Approximate description of internal Faraday dispersion

An important consequence of internal Faraday dispersion is that it also introduces asymmetry along the line of sight because less polarized emission is observed from deeper layers of the source than from nearer ones. As a result, polarization properties of even a symmetric slab resemble those of an asymmetric source.

In the case of internal Faraday dispersion the following approximation can be applied: assume that the polarized emission observed originates completely in the near part of the source where the amount of Faraday depolarization due to a random magnetic field and fluctuations in electron density is small. Then the random component is completely neglected in the near part of the source, and the degree of polarization and Faraday rotation measure are estimated from the corresponding expressions for differential Faraday rotation in a purely regular magnetic field applied to the part of the source that is visible in polarized emission. (Clearly, this approximation breaks down at such long wavelengths that the thickness of the visible layer becomes comparable to the cell size – see Section 6.3.1.) This approximation, which may be called the approximation of an *'opaque layer'*, is useful because it is often difficult to analyse consistently the *complex* polarization of a synchrotron source; instead, most authors consider separately the degree of polarization and Faraday rotation measure. The opaque-layer approximation may be an appropriate step in attempts to combine these two parameters of polarization in a consistent interpretation.

Such an approach was used by Berkhuijsen et al. (1997) who analysed the regular magnetic field in M51 by considering the polarization angles measured at four wavelengths, $\lambda\lambda$2.8, 6.3, 18.0 and 20.5 cm. To simplify their analysis, they used the observed degree of polarization to estimate the geometrical depth in the thermal disc of the galaxy beyond which the synchrotron emission is completely depolarized by internal Faraday dispersion. After that they assumed that the observed polarization angles are determined by the regular field alone in the upper layer of the galaxy visible in the polarized emission. In this section we discuss the accuracy of this approximation.

This approximation is equivalent to replacing equation (32) by the following expression:

$$\langle \mathcal{P} \rangle = \tfrac{1}{2}\langle \mathcal{P}_0 \rangle \int_{z_*/h_\varepsilon}^{z_b/h_\varepsilon} \mathrm{d}s\, F(|s|) \exp\left[\mathrm{i}\lambda^2 \mathcal{R} \int_{s/q}^{z_b/h_M} f(|t|)\, \mathrm{d}t \right], \qquad (35)$$

where z_* is defined as the geometric depth at which the variance of Faraday rotation due to the random field [i.e. the term neglected in equation (35)] is equal to a certain value ϕ_* (of order unity) which can be adjusted to control the accuracy of the approximation:

$$\lambda^4 \sigma_{\mathrm{RM}}^2 q_m \int_{z_*/h_M}^{z_b/h_M} g(q_m|t|)\, dt = \phi_* \,. \qquad (36)$$

For a given ϕ_*, this condition can be met only for $\lambda \geq \lambda_*$, where $\lambda_*^4 = \phi_*/(2\sigma_{\mathrm{RM}}^2)$. For $\lambda < \lambda_*$ internal Faraday dispersion can be completely neglected and the results of Section 3.2 are expected to provide a good approximation. Thus, for $\lambda < \lambda_*$, equation (35) should be applied with $z_* = -z_b$.

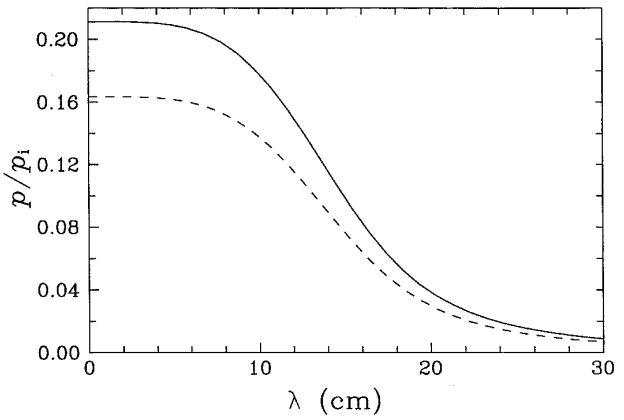

Figure 6. A description of internal Faraday dispersion in terms of the opaque-layer approximation. Exact results for a symmetric Gaussian slab with the same parameters as in Fig. 4 are shown solid, and approximate results obtained from equation (35) with $\phi_* = 1$ in equation (36) are shown dashed. (a) The degree of polarization, (b) the polarization angle and (c) the corresponding values of RM. The discontinuity in the approximate dependences occurs at $\lambda = \lambda_*$.

For $\lambda \geq \lambda_*$, internal Faraday dispersion completely depolarizes the emission from the far part of the slab, $z < z_*$, and already at $\lambda_{1/2} = 2^{1/4}\lambda_*$ the polarized emission originating in the half of the slab at $z < 0$ does not contribute to equation (35), i.e. $z_* = 0$. For $\sigma_{\mathrm{RM}}^2 = 10^3\ \mathrm{rad}^2\ \mathrm{m}^{-4}$, we have $\lambda_* \approx 15\phi_*^{1/4}$ cm and $\lambda_{1/2} \approx 18\phi_*^{1/4}$ cm.

For a Gaussian slab, the integral in equation (36) reduces to the error function, which gives the following equation for z_*:

$$\mathrm{erf}\,(\sqrt{2}z_*/h_\varepsilon) = 1 - \left(\lambda_*/\lambda\right)^4 \quad \text{for} \quad \lambda \geq \lambda_*.$$

Fig. 6 demonstrates that the opaque-layer approximation well describes basic qualitative features of both p and Ψ at short and moderate λ, although the accuracy is rather poor for RM. The approximation is shown for $\phi_* = 1$. For any given value of ϕ_* the relative accuracy of the approximation is different for p and Ψ: for larger ϕ_*, Ψ is approximated better, whereas p is estimated more accurately for smaller values of ϕ_*. Values of ϕ_* in the range $0.5 \leq \phi_* \leq 1$ appear to be optimal. We should note a peculiar feature of the exponential slab, for which the approximate expression (35) yields RM $\equiv 0$ for $\lambda > \lambda_{1/2}$.

We conclude that the opaque-layer approximation, which assumes that internal Faraday dispersion makes the far side of the source invisible in polarized emission, yields a reasonable approximation to p and Ψ, but not to RM. The accuracy is generally within $10°$–$20°$ for Ψ at $\lambda \lesssim 20$ cm, which is about the typical observational error. Therefore interpretations of observed polarization patterns that use this approximation should be formulated in terms of observed polarization angles Ψ rather than in terms of observed Faraday rotation measure. However, this approximation becomes inapplicable at longer wavelengths, typically those exceeding $\lambda\lambda$25–30 cm.

6.3.1 *Extreme internal Faraday dispersion*

In an extreme case of strong internal Faraday dispersion, only an upper layer of turbulent cells (which is the closest to the observer) contributes to the observed polarized emission. Then the polarization pattern will be completely random, but the degree of polarization can be significant. As can be seen from equation (A3),

the random contribution of the upper layer of turbulent cells at $z_b - z \lesssim l_m$ to the observable polarized emission can be considerable at long wavelengths where depolarization within a single correlation cell of m is significant. Assuming that the field is uniform within a cell, we see that this occurs when $\sigma_m l_m \lambda^2 \gtrsim 1$. A typical degree of polarization at $\lambda^2 \gtrsim (\sigma_m l_m)^{-1}$ is equal to $N_W^{-1/2}$. Under conditions typical of galactic discs, the contribution of the upper layer is important at $\lambda \gtrsim 35\,\mathrm{cm}$ for $n = 0.03\,\mathrm{cm}^{-3}$, $\sigma_z = 5\,\mu\mathrm{G}$ and $l_m = 100\,\mathrm{pc}$ with σ_z the rms value of the line-of-sight random magnetic field.

Significant polarization from a thin layer in the source close to the observer may possibly explain significant polarization at $\lambda \approx 90\,\mathrm{cm}$ observed in the halo of NGC 891 by De Breuck et al. (in preparation), where $n = 0.003\,\mathrm{cm}^{-3}$ and $l_m = 1000\,\mathrm{pc}$ are plausible estimates, so that the fluctuations become strong at $\lambda \gtrsim (\sigma_m l_m)^{-1} \simeq 65\,\mathrm{cm}$.

7 COMMENTS ON EXTERNAL FARADAY DISPERSION

A distinct depolarization mechanism is the depolarization in an external Faraday screen, i.e. a magneto-ionic region devoid of relativistic electrons which is located between the source of synchrotron emission and the observer. Owing to Faraday rotation by a random magnetic field, the plane of polarization undergoes a random walk which leads to depolarization as long as many turbulent cells are within the beam area. This effect is physically similar to internal Faraday dispersion, but it requires a separate treatment because depolarization occurs at positions where the synchrotron emissivity has vanished. A comprehensive treatment of Faraday depolarization in an external screen can be found in Burn (1966) and Tribble (1991). In Appendix B we review their results in terms of the present formalism.

An important peculiarity of a Faraday screen is that the mean degree of polarization, given by equation (B3) of Appendix B, decreases with λ as $|\langle \mathcal{P}_{ex} \rangle| \propto \exp(-2\sigma_{RM}^2 \lambda^4)$, whereas fluctuations of the complex polarization, equations (B4) and (B6), decrease only as $\sigma_{\mathcal{P}_{ex}} \propto (\sigma_{RM}\lambda^2)^{-1}$, where σ_{RM} is defined in equation (31). Therefore the fluctuations can become dominant at relatively small λ, resulting in a power-law variation of the observed degree of polarization with λ. In agreement with this conclusion, Johnson et al. (1995) noted that in their sample of radio sources, where depolarization is due to foreground Faraday rotation, p does not decrease exponentially with λ^4.

Equations (B3) and (B6) essentially rely on the Gaussian statistical properties of the fluctuations of m, since they were obtained using equation (5) of Appendix A. The Gaussian approximation cannot be applied to a geometrically thin Faraday screen (i.e. $z_b - z_\varepsilon \lesssim l_m$) if the random magnetic field is assumed to be uniform within correlation cells having independent directions and strengths in different cells. Then fluctuations in the polarization angle (and the complex polarization itself) are completely correlated at the exit from the source for separations smaller than l_{RM}, and completely uncorrelated otherwise. In other words, the transverse correlation length of $\mathcal{P}_{ex}$, denoted as $l_{\mathcal{P}}$, is equal to the transverse correlation length of RM, $l_{\mathcal{P}} = l_{RM}$ for such a screen. Meanwhile, $l_{\mathcal{P}} \ll l_{RM}$ for a Gaussian random screen, equation (B5). Note that $l_{\mathcal{P}}$ and l_{RM} remain different from each other for a *thick* screen with the same cell model for the random magnetic field, because each line of sight passes through many correlation cells and equation (B6) remains applicable.

We stress that the Gaussian statistical properties of a random field and its spectral properties refer to different physical characteristics of the field: for example, one can envisage a Gaussian random field with both extended and single-scale spectra. Tribble (1991) discussed the role of a range of scales of magnetic fluctuations. An extended power-law spectrum of magnetic fluctuations leads to a power-law behaviour of the autocorrelation function of p. However, the power-law behaviour in Tribble's expression for the observable degree of polarization, equation (B6), arises not from spectral properties of the fluctuations but from the fact that the filling factor of the regions, which contribute significantly to the observable degree of polarization, is a function of wavelength (see Appendix B for details).

A power-law form of the autocorrelation function can be important for studies of the fine structure of the magneto-ionic medium in the Milky Way. However, the resolutions available for observations of external galaxies are as yet insufficient to admit extensive studies of the spectral properties of magneto-ionic fluctuations.

7.1 Some applications

For illustration, consider the halo of an external galaxy illuminated by a synchrotron-emitting disc (i.e. seen almost face-on), adopting the following parameters for the halo: $b = 2\,\mu\mathrm{G}$, $n = 3 \times 10^{-3}\,\mathrm{cm}^{-3}$, $l_{RM} = 500\,\mathrm{pc}$, $L = z_b - z_\varepsilon = 5\,\mathrm{kpc}$. For these values of parameters [with L replacing $2h_m$ in equation (31)], we obtain $\sigma_{RM} \approx 8\,\mathrm{rad\,m^{-2}}$. Hence the contribution of the fluctuation term (B4) to the degree of polarization is smaller than that of the mean value (B3) at $\lambda < 20\,\mathrm{cm}$, provided that the beam size is large enough, $D \gtrsim 2\,\mathrm{kpc}$, or the number of turbulent cells in the beam cylinder is $N \gtrsim 40$. In our Galaxy, Leahy (1987) found $\sigma_{RM} \approx 20\,\mathrm{rad\,m^{-2}}$ within 10° from the Galactic plane and $\sigma_{RM} \approx 6\,\mathrm{rad\,m^{-2}}$ near the Galactic North Pole. Therefore the interstellar gas does not impose excessively strong fluctuations on the radio emission of high-latitude extragalactic radio sources.

Towards the lobes of radio galaxies embedded in clusters, RM values of several $1000\,\mathrm{rad\,m^{-2}}$ have been observed (Dreher et al. 1987; Taylor et al. 1990, 1994; Carilli et al. 1997). This is interpreted as the effect of the hot intracluster gas with $B \simeq 5\,\mu\mathrm{G}$, $n \simeq 2 \times 10^{-2}\,\mathrm{cm}^{-3}$ and $L \simeq 20\,\mathrm{kpc}$. In such cases, Faraday depolarization is dominated by RM gradients (see Section 8.2).

Deviations from Gaussian statistical properties of $\exp(-2\sigma_{RM}^2\lambda^4)$ are expected to become significant when $2\sigma_{RM}^2\lambda^4 \gg 1$. In our case $2\sigma_{RM}^2\lambda^4 \approx 0.2$ at $\lambda = 20\,\mathrm{cm}$ for the halo parameters adopted above, so that the Gaussian statistics provide a reasonable description of the depolarization.

8 GRADIENTS IN RM ACROSS THE BEAM

In this section we discuss depolarization arising from a resolved or unresolved gradient of Faraday rotation measure across the beam, originating in the synchrotron source (as in spiral galaxies) and in a foreground screen (as in the case of radio galaxies).

8.1 RM gradients in a synchrotron source

Berkhuijsen & Beck (1990) measured polarization in the south-western arm of M31 at wavelengths of λλ6.3 and 20.1 cm at a resolution of 600 pc × 3000 pc along the major and minor axes, respectively. They found systematic variations in RM giving rise to gradients in RM across the beam. They noted that the ratio of the degrees of polarization at the two wavelengths, known as depolarization $\mathrm{DP}_{20/6} = p(20.1\,\mathrm{cm})/p(6.3\,\mathrm{cm})$, systematically decreases

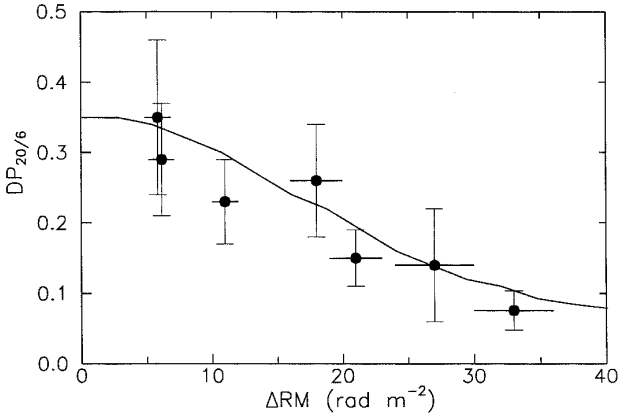

Figure 7. Depolarization, defined as the ratio of the degrees of polarization at λλ20.1 and 6.3 cm, in the south-western arm of M31 as a function of the difference in RM across the beam (points with error bars – Berkhuijsen & Beck 1990), and the fitted dependence given by equation (38) with $\sigma^2_{\rm RM} = 840\,{\rm rad^2\,m^{-4}}$ and ${\rm RM}_0 = 0$.

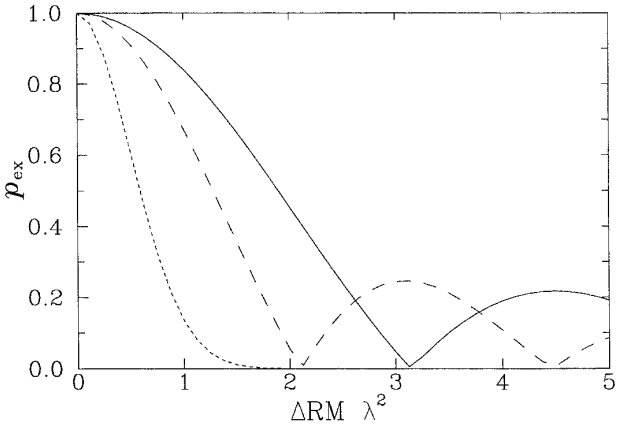

Figure 8. Degree of polarization in a foreground Faraday screen with a gradient of RM as given by equations (39) and (42) for a Gaussian beam with $x_0 = \frac{1}{2}D$ (solid, model A), by equation (41) for a flat beam profile with $x_0 = \frac{1}{2}D$ (dashed, model C), and by equation (40) for a Gaussian beam with $x_0 \to \infty$ (dotted, model B), where $2x_0$ is the lateral extent of the region with a gradient of RM and D is the beam diameter.

with increasing gradient in RM across the beam. The data used were slightly oversampled, with the separation between the measured points being equal to about one-third of the beam size. Their results are reproduced in Fig. 7.

To describe the effects of RM varying systematically across the beam, we consider a synchrotron-emitting region with a linear gradient of Faraday rotation measure across the beam,

$$\mathrm{RM} = \mathrm{RM}_0 + \Delta\mathrm{RM}\, x/D\,, \tag{37}$$

where x is measured across the beam, $|x| \le x_0$, D is the beam diameter, and ΔRM is the variation in RM across the beam. It is assumed that RM = constant for $|x| > x_0$.

For a flat beam profile, $w = 1$, the complex polarization is given by equation (13), where we have to evaluate $\left\langle \exp 2{\rm i}K\lambda^2 \int_z^{z_{\rm b}} n\overline{B}_z\, {\rm d}z' \right\rangle_{W\times h}$ for $\mathrm{RM} = \frac{1}{2}Kn\overline{B}_z L$ given by equation (37). As averaging over the volume $W \times h$ reduces to averaging over x, the result has the form

$$\mathcal{P} = \tilde{\mathcal{P}} \int_0^1 \exp\left(4{\rm i}\,\mathrm{RM}_0\,\lambda^2 s\right) \frac{\sin\left(2\Delta\mathrm{RM}\,\lambda^2 s\right)}{2\Delta\,\mathrm{RM}\,\lambda^2 s}\,{\rm d}s\,, \tag{38}$$

where $\tilde{\mathcal{P}}$ is the average value of the complex polarization across the beam at ΔRM = 0 and the integration variable was introduced as $s = 1 - z/z_{\rm b}$, with $2z_{\rm b} = L$ the full extent of the region along the line of sight. One can use equation (38) for both resolved ($x_0 \ge D$) and unresolved ($x_0 < D$) gradients.

As argued by Berkhuijsen & Beck (1990), depolarization by differential Faraday rotation is unimportant in the observed region of M31, so that we can neglect RM_0. The amount of depolarization at ΔRM = 0, denoted $\tilde{\mathcal{P}}$ in equation (38), should be adjusted to the value $\mathrm{DP}_{20/6} = 0.35$ observed in regions where the gradient of RM is negligible. Assuming that this value is due to internal Faraday dispersion, described by equation (34), this requires a reasonable value $\sigma^2_{\rm RM} \approx 840\,{\rm rad^2\,m^{-4}}$. The result of applying equation (38) is shown in Fig. 7. Thus we obtain a rather satisfactory fit to the depolarization data for a range of ΔRM by adjusting only a single parameter, $\sigma_{\rm RM}$, to fit $\mathrm{DP}_{20/6}$ at ΔRM = 0.

8.2 RM gradients in a foreground screen

In the Faraday screen in front of the lobes of radio galaxies embedded in a cluster, RM gradients of up to $2000\,{\rm rad\,m^{-2}}$ over 1 arcsec have been observed (Dreher et al. 1987; Taylor et al. 1990, 1994), causing strong depolarization when using low angular resolution. In this section we obtain an explicit expression for depolarization arising from a gradient of RM in a foreground Faraday screen.

We consider three models: (A) a Gaussian beam and an arbitrary transverse variation of RM in a finite region $|x| \le x_0$; (B) a Gaussian beam and an infinite transverse extent of a linear variation of RM (a model identical to that of Johnson et al. 1995); and (C) a flat beam profile and a linear RM variation in a finite region.

Using equation (B2) for the Gaussian beam, $w = (2\sqrt{2\pi}/D)\exp(-2r^2/D^2)$, we obtain for model A

$$\mathcal{P}_{\rm ex} = \frac{2\sqrt{2\pi}}{D} \int_{-x_0}^{x_0} \exp\left[-\frac{2x^2}{D^2} + 2{\rm i}\mathrm{RM}(x)\lambda^2\right] {\rm d}x\,, \tag{39}$$

where $\mathrm{RM} = KnB_z(z_{\rm b} - z_\varepsilon)$. This expression is applicable for any relation between x_0 and D.

In model B, the result of Johnson et al. (1995) is obtained from equation (39) if we suppose that the linear gradient (37) extends from $x = -\infty$ to $x = \infty$, i.e. $x_0 \to \infty$ (a resolved gradient):

$$\begin{aligned}\mathcal{P}_{\rm ex} &= 2\frac{\sqrt{2\pi}}{D}\,{\rm e}^{2{\rm i}\mathrm{RM}_0\lambda^2} \int_{-\infty}^{\infty} \exp\left(-2\frac{x^2}{D^2} + {\rm i}\Delta\mathrm{RM}\,\lambda^2\,\frac{x}{D}\right){\rm d}x \\ &= \exp\left[2{\rm i}\mathrm{RM}_0\,\lambda^2 - 2(\Delta\mathrm{RM}\,\lambda^2)^2\right]\,. \end{aligned} \tag{40}$$

Another simple result is obtained for a flat beam profile $w = 1$, model C. Then, using equation (37), we have from equation (B2)

$$\mathcal{P} = \mathcal{P}_{\rm int} \exp\left(2{\rm i}\mathrm{RM}_0\,\lambda^2 - 2\sigma^2_{\rm RM}\,\lambda^4\right) \frac{\sin\Delta\mathrm{RM}\,\lambda^2}{\Delta\,\mathrm{RM}\,\lambda^2}\,, \tag{41}$$

where the additional effect of the random field is also included (the term with $\sigma_{\rm RM}$).

The three models are compared in Fig. 8 where we show $p_{\rm ex} = |\mathcal{P}_{\rm ex}|$ as a function of $\Delta\mathrm{RM}\,\lambda^2$. The solid line was obtained by direct integration of equation (39) with

$$\mathrm{RM}(x) = \frac{1}{\pi}\Delta\mathrm{RM}\arctan\frac{x}{x_0} \tag{42}$$

and $x_0 = \frac{1}{2}D$. We also plotted results from equation (40) (dotted) and equation (41) (dashed) which are both devised to approximate

equation (39). In model A, as in its approximation model C, a gradient of RM leads to similar non-monotonic variations of the degree of polarization with $\Delta\mathrm{RM}\,\lambda^2$. In contrast, $p_{\rm ex}$ monotonically decreases in model B.

We conclude that equation (40) is not a good approximation to equation (39) and is applicable only to resolved gradients of RM. It cannot be applied to unresolved or partly resolved gradients. For them, equation (41) is a fair approximation to equation (39).

The formula of Johnson et al. (1995) strongly underestimates the degree of polarization for a given ΔRM. A quantitative agreement between equation (40) and the exact result (39) can be reached for $\Delta\mathrm{RM}\,\lambda^2 \lesssim 1$ if we replace the coefficient $1/\pi$ in equation (42) by $4/\pi$. On the other hand, a good agreement between equations (39) and (41) for *any* value of $\Delta\mathrm{RM}\,\lambda^2$ is reached when $1/\pi$ is replaced by $1.35/\pi$ in equation (42). Thus the simple equation (41) can be used even for a Gaussian beam provided only that a correction factor of 1.35 is introduced into the resulting estimate of the RM gradient.

9 ANOMALOUS DEPOLARIZATION EXPLAINED BY A TWISTED MAGNETIC FIELD

Observations of nearby galaxies at wavelengths of λλ18 and 20 cm have revealed regions of anomalous depolarization where p at the longer wavelength is larger than that at the shorter one. In terms of depolarization between different wavelengths, defined as $\mathrm{DP}_{20/18} = p(20\,\mathrm{cm})/p(18\,\mathrm{cm})$, these regions have $\mathrm{DP}_{20/18} > 1$. Typical values of $\mathrm{DP}_{20/18}$ are 1.2–1.5, but locally values as high as 3 are reached. This was observed in e.g. M51 (Horellou et al. 1992) and NGC 6946 (Beck 1991). At low resolutions, the regions of anomalous depolarization appear to be extended – a strip across the whole image of M51 and a complete quadrant of the image of NGC 6946. However, the maps at the full resolution of 42 arcsec (unpublished) reveal a patchy pattern with $\mathrm{DP}_{20/18} > 1$ only in isolated regions of about 1–2 kpc in size.

As the size of the regions with anomalous depolarization far exceeds the anticipated correlation scale of the random magnetic field, it appears that this phenomenon is connected with some specific properties of the regular magnetic fields. The simplest explanation invokes differential Faraday rotation. If the first zero of the degree of polarization in equation (3) occurs at $\lambda \lesssim 18$ cm, p grows with λ in a relatively narrow range of wavelengths between λλ18 and 20 cm. Then depolarization exceeding unity, DP > 1, would occur only in this wavelength range, whereas normal values DP < 1 would be observed at shorter wavelengths (see Fig. 1). This explanation requires that internal Faraday dispersion negligibly affects p (because it removes the mimina in Fig. 1), which is unlikely.

Anomalous depolarization could also be due to a partially resolved or unresolved foreground gradient of RM in the galactic halo because then p is a non-monotonic function of λ (see Section 8.2 and Fig. 8). The difficulties with this explanation are the same as in the case of differential Faraday rotation just discussed.

We suggest that the anomalous depolarization may result from a specific geometric configuration of the regular magnetic field which may be typical of spiral galaxies. Consider a regular magnetic field with a line-of-sight component that is uniform and a transverse component that changes its direction along the line of sight, z. Twisted magnetic fields are a natural consequence of the fact that the azimuthal and radial components of the field generated by the galactic dynamo exhibit different variations across the disc (Ruzmaikin, Shukurov & Sokoloff 1988) or of a reversal between the disc and the halo of a galaxy (Sokoloff & Shukurov 1990; Brandenburg, Moss & Shukurov 1995).

In a twisted magnetic field, the intrinsic polarization angle ψ_0 varies along z. If the Faraday rotation of the plane of polarization is equal to the variation in ψ_0, the outcoming polarized emission will *not* be depolarized at all. It is clear that this may occur only at a single wavelength. On the other hand, the degree of polarization at short wavelengths can be smaller or even vanish in a twisted transverse field. For a linear variation of ψ_0 with z, $p = 0$ at $\lambda \to 0$ for $\Delta\psi_0 = 180°$, where $\Delta\psi_0$ is the variation in ψ_0 along the line of sight. As a result, in a twisted field p is an increasing function of λ for a wide range of wavelengths, which means that DP > 1. Since the wavelength range in which the anomalous depolarization occurs can be rather wide in a region occupied by twisted magnetic field, the regions with DP > 1 can be extended and their appearance does not require any exact adjustment of parameters.

To illustrate the effect of a twisted magnetic field, consider the simplest case of a slab $|z| \le z_{\rm b}$ with $\psi_0 = \Delta\psi_0\, z/(2z_{\rm b})$, where $\Delta\psi_0$ is the increment in ψ_0 across the slab. For a uniform $\overline{B}_z$ we have from equation (1):

$$\mathcal{P} = p_{\rm i}\frac{1}{2z_{\rm b}}\int_{-z_{\rm b}}^{z_{\rm b}} \exp{\rm i}\left[\Delta\psi_0\frac{z}{z_{\rm b}} + \mathcal{R}\lambda^2\left(1-\frac{z}{z_{\rm b}}\right)\right]{\rm d}z$$

$$= p_{\rm i}\frac{\sin(\Delta\psi_0 - \mathcal{R}\lambda^2)}{\Delta\psi_0 - \mathcal{R}\lambda^2}\exp{\rm i}\mathcal{R}\lambda^2\,, \qquad (43)$$

where $\mathcal{R} = 2Kn\overline{B}_z z_{\rm b}$. It is clear that for a linear twist the degree of polarization monotonically grows with λ for

$$\lambda^2 < \Delta\psi_0/\mathcal{R}\,, \qquad (44)$$

in which wavelength range the anomalous depolarization occurs. For $\Delta\psi_0 = 180°$ and $\mathcal{R} = 30\,\mathrm{rad\,m^{-2}}$, we have DP > 1 for $0 < \lambda \le 32$ cm.

We note that anomalous depolarization also occurs if ψ_0 changes abruptly between two homogeneous layers. However, in this case the effect is strongest for $\Delta\psi_0 = 90°$, as follows from equation (10).

A specific feature of anomalous depolarization in a twisted field is that it occurs over a wide range of wavelengths, including very small ones. This property can be used to distinguish it from effects caused by differential Faraday rotation (Section 3).

We should note that anomalous depolarization between λλ18 and 20 cm is observed in galaxies seen almost face-on. The line-of-sight magnetic field is then quite weak, so that the value $\mathcal{R} = 30\,\mathrm{rad\,m^{-2}}$ adopted in the above example after equation (44) is justified. In M31, which is seen at a high inclination, the line-of-sight magnetic field may be stronger. Here some traces of anomalous depolarization are observed at significantly shorter wavelengths, λλ6 and 11 cm (Berkhuijsen et al. 1987). The tendency of the anomalous depolarization to occur at shorter wavelengths when $\mathcal{R}$ grows agrees with equation (44).

Random magnetic fields make this effect weaker because their line-of-sight component shifts the maximum in p to smaller wavelengths owing to Faraday dispersion. We illustrate polarization in a twisted magnetic field and the effects of random magnetic fields in Fig. 9.

In the thin-disc dynamo model of Krasheninnikova et al. (1989), ψ_0 changes from about $-20°$ at the mid-plane to positive values above about $0.8h$ with h the disc half-thickness. This amount of twist is smaller than the optimum value of 180°. A twist comparable to the optimum value can be associated with a smooth reversal of

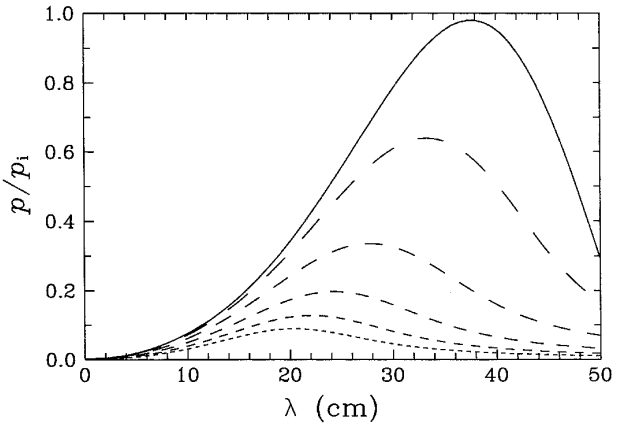

Figure 9. The degree of polarization in a slab hosting a twisted magnetic field with ψ_0 changing linearly from 0° to 180° along the line of sight. Shown are the results for a purely regular magnetic field with $\mathcal{R} = 22\,\mathrm{rad\,m^{-2}}$ [solid – this is described by equation (43)] and for several values of the superimposed random magnetic field corresponding to $\sigma_{\mathrm{RM}} = 5.2$, 10.4, 15.6, 20.8 and $26.0\,\mathrm{rad\,m^{-2}}$ (dashed curves from top to bottom).

magnetic field between the disc and the halo of a spiral galaxy (Sokoloff & Shukurov 1990; Brandenburg et al. 1995), which was detected in M51 by Berkhuijsen et al. (1997). In this case $\Delta\psi_0$ is close to its optimum value of 180°. However, the decrease in the synchrotron emissivity with height may hamper this effect. A more detailed comparison with observations will be given elsewhere.

Urbanik, Elstner & Beck (1997) explain the anomalous depolarization in NGC 6946 by a helical shape of the magnetic field lines in this galaxy. A helical field seen at an angle to its symmetry axis represents a particular case of a twisted field, so that this mechanism may be related to that discussed above.

Other cases in which a twisted magnetic field is natural to expect are jets in active galaxies and near young stars where helical magnetic fields are believed to be widespread.

10 SMALL FILLING FACTORS

So far we have implicitly assumed that the filling factors of both relativistic electrons and magneto-ionic material are close to unity. This assumption may not be valid if, say, H II regions make a significant contribution to the depolarization or the magnetic field is concentrated to thin flux ropes.

Consider a two-component magneto-ionic plasma consisting of clouds of a size d (having uncorrelated magnetic fields) embedded in a diffuse medium with a regular magnetic field. The diffuse component has an extent L along the line of sight and an intrinsic Faraday rotation measure $\mathcal{R}$. The clouds have a volume filling factor f_V, and a high value of $\sigma_{\mathrm{RM}} = Kn\sigma_z(dL)^{1/2}$. The surface filling factor of the clouds is given by $f_W = f_V L/d$ and is not restricted to be smaller than unity. If $f_W \gtrsim 1$, the two-component nature of the magneto-ionic medium can be taken into account by replacing σ_{RM} by $f_V^{1/2}\sigma_{\mathrm{RM}}$ in the formulae given above because $\langle nb_z\rangle^2 = f_V\langle(nb_z)^2\rangle$. However, f_W is no longer close to unity when $f_V \lesssim d/L$. In this case a significant portion of polarized emission avoids the dense clouds and is sensitive to $\mathcal{R}$ alone. At long wavelengths, $2\sigma_{\mathrm{RM}}^2\lambda^4 \gtrsim 1$, where the emission from the ensemble of dense clouds is completely depolarized, the diffuse component alone determines the polarization properties of the synchrotron emission.

For example, consider the interpretation of observations of NGC 6946 by Ehle & Beck (1993), who considered small clouds with $d \approx 1$ pc and $f_V \approx 0.05$ within a thin disc of about 100-pc full thickness. Their surface filling factor, $f_W \simeq 5$, significantly exceeds unity, with the implication that this component of the interstellar medium can be well described using the above formulae.

11 DISCUSSION AND CONCLUSIONS

We have discussed various mechanisms that determine complex polarization under conditions typical of spiral galaxies. Some of our conclusions are also applicable to radio galaxies and other extended radio sources. A major part of the available observations of galaxies has been performed at wavelengths of about λ20 cm where the objects are Faraday-thick. This strongly complicates the interpretation (although does not make it impossible). Therefore we have restrained ourselves here from consistent interpretation of any such observations and, instead, illustrated individual physical effects using isolated observational examples. Wherever possible, we have discussed how individual effects combine with each other; such combinations are often non-trivial. In Section 9 we have discussed an example of the application of our results using a model of twisted magnetic field that illustrates how simple magnetic configurations can lead to very unusual polarization patterns.

In order to isolate and concentrate on generic behaviours, we have considered mainly analytically solvable models. In the case of regular magnetic fields, polarization properties of an object can be easily calculated for any given magnetic field and electron density distribution. However, one should be careful with modelling the magneto-ionic medium because the complex polarization is sensitive to such delicate properties as the symmetry and the relations between the scaleheights of the constituents of the medium.

The situation is much more complicated in the case of polarization in a random magnetic field. In this case straightforward integration in equation (1) is practically impossible, merely because one can never know exact realizations of the random fields involved. Therefore one has to adopt plausible assumptions about statistical properties of n and $\boldsymbol{B}$ and to perform analytical integration (averaging) of the random functions. This yields simpler integral expressions of the type (30) and (B3). If even averaged properties of the source are not known in sufficient detail, further assumptions should be involved and expressions similar to equation (33) become useful.

More generally, the purpose of any interpretation is to deduce the physical parameters of the source from its polarized emission (the inverse problem), rather than to calculate the complex polarization for a given magneto-ionic medium. However, the formulation of and approaches to the inverse problem go far beyond the scope of this paper, although our results may be useful in this respect.

Our results may be summarized as follows.

(1) Depolarization effects occurring within the synchrotron source in a magneto-ionic medium with a purely *regular* magnetic field are discussed in Sections 3.1 to 3.4. In this case differential Faraday rotation leads to wavelength-dependent depolarization of radio synchrotron emission.

(i) Burn's formula, equation (3), is applicable not only to a single uniform magneto-ionic layer but also to a non-uniform (e.g. exponential) layer, either symmetric or asymmetric, as long as the intrinsic polarization angle is constant along the line of sight (z) and the quantities $n\overline{B}_z$ and ε have identical dependences on z, and differ by only a (dimensional) numerical factor.

(ii) However, the relation between the observable degree of polarization p and the observable Faraday rotation measure RM differs from Burn's formula in the case of *any* non-uniform distribution of $n\overline{B}_z$, in the sense that p is generally smaller (i.e. *stronger* depolarization) than predicted by Burn's formula from the observable RM (see Figs 1 and 3).
(iii) For an asymmetric distribution, RM varies with wavelength λ and may even reverse its sign at some wavelength, although the magnetic field has no reversals (Fig. 2).
(iv) In a multi-layer slab (with or without reversals), both p and RM may vary strongly with λ (see also Fig. 2). The total RM, obtained from equation (11), can be a complicated function of the RMs in the sublayers.

(2) Depolarization effects caused by *random* magnetic fields are discussed in Sections 4 to 5.2.

(i) Random magnetic fields in a synchrotron source lead, in particular, to wavelength-independent depolarization. We give the general formula for wavelength-independent depolarization (equation 18) which, for a large number of correlation cells, is identical to Burn's result for an isotropic random field and synchrotron emissivity ε proportional to $B_\perp^2$. It generalizes Laing's (1981) result for polarization in an anisotropic random magnetic field by including a regular magnetic field. In the case of equipartition between the energy densities of cosmic rays and magnetic fields ($\varepsilon \propto B^2 B_\perp^2$) (see Section 5.2), the predicted degree of polarization at $\lambda \rightarrow 0$ is up to 50 per cent larger than in the standard case (see Fig. 4).
(ii) Random fields in a synchrotron-emitting layer containing thermal electrons lead to wavelength-dependent depolarization (internal Faraday dispersion) and always to a wavelength-dependent RM. As λ increases, the layer becomes opaque for polarized emission, causing a reduced observable RM. We show that the approximation of a depolarized far side and a visible near side of the layer reasonably describes $p(\lambda)$ and $\psi(\lambda)$, but not RM(λ) (see Fig. 6).
(iii) The contribution of the upper layer of turbulent cells to the observed polarized emission can be considerable at long wavelengths. Therefore strong fluctuations in $p(\lambda)$ are expected for the synchrotron emission from galactic discs and haloes at long wavelengths; typical values of p can be significantly larger than the mean value expected from the standard formulae. This may explain recent observations in NGC 891 at λ90 cm (see Section 6).
(iv) Random fields in a magneto-ionic medium between the synchrotron source and the observer (external Faraday dispersion) also lead to wavelength-dependent depolarization. The fluctuations in the degree of polarization may become dominant and observable at $\lambda \gtrsim 20$ cm (see Section 7).

(3) Faraday depolarization caused by RM gradients across the beam can be described by equation (38) when they occur within the synchrotron source, in good agreement with observations in M31 (see Fig. 7). For RM gradients in a foreground screen, equation (41) provides a reasonably accurate description.

(4) Anomalous depolarization with p increasing with wavelength can be explained by the proximity of the wavelength of observations to a minimum in p produced by differential Faraday rotation. This explanation requires that internal Faraday dispersion negligibly affects p, which is unlikely. We therefore propose another explanation (see Fig. 9), based on a regular magnetic field having a twist along the line of sight. Such a configuration may arise in the transition layer between the disc and the halo of a galaxy, and may possibly explain the anomalous depolarization observed in NGC 6946 between $\lambda\lambda$18 and 20 cm.

ACKNOWLEDGMENTS

AS, ADP, AAB and DDS are grateful to the Deutsche Forschungsgemeinschaft for financial support for several visits to the MPIfR Bonn, and to R. Wielebinski for hospitality. We acknowledge stimulating comments from the anonymous referee which helped to refine our results and to improve the presentation. Financial support from PPARC, the Russian Foundation for Basic Research under grants 96–02–16252a and 95–01–01284a, NATO collaborative research grant CRG1530959 and a joint grant RFBR/DFG 96–02–00094G is acknowledged. We also thank Dr M. Krause for helpful discussions. We also acknowledge financial support from the Royal Society, the University of Newcastle, and the Particle Physics and Astronomy Research Council (UK).

REFERENCES

Beck R., 1991, A&A, 251, 15
Beck R., Brandenburg A., Moss D., Shukurov A., Sokoloff D., 1996, ARA&A, 34, 153
Berkhuijsen E. M., Beck R., 1990, in Beck R., Kronberg P. P., Wielebinski R., eds, Proc. IAU Symp. 140, Galactic and Intergalactic Magnetic Fields. Kluwer, Dordrecht p. 201
Berkhuijsen E. M., Beck R., Gräve R., 1987, in Beck R., Gräve R., eds, Interstellar Magnetic Fields. Springer, Berlin, p. 38
Berkhuijsen E. M., Golla G., Beck R., 1991, in Bloemen H., ed., Proc. IAU Symp. 144, The Interstellar Disk–Halo Connection in Galaxies. Kluwer, Dordrecht p. 233
Berkhuijsen E. M., Horellou C., Krause M., Neininger N., Poezd A. D., Shukurov A., Sokoloff D. D., 1997, A&A, 318, 700
Beuermann K., Kanbach G., Berkhuijsen E. M., 1985, A&A, 153, 17
Bologna J. M., McClain E. F., Sloanaker R. M., 1969, ApJ, 156, 815
Brandenburg A., Moss D., Shukurov A., 1995, MNRAS, 276, 651
Burch S. F., 1979, MNRAS, 186, 519
Burn B. J., 1966, MNRAS, 133, 67
Carilli C. L., Röttgering H. J. A., van Oijk R., Miley G. K., van Breugel W. J. M., 1997, ApJS, 109, 1
Chi X., Young E. C. M., Beck R., 1997, A&A, 321, 71
Cioffi D. F., Jones T. W., 1980, AJ, 85, 368
Dickey J. M., Lockman F. J., 1990, ARA&A, 28, 215
Donner K. J., Brandenburg A., 1990, A&A, 240, 289
Dreher J. W., Carilli C. L., Perley R. A., 1987, ApJ, 316, 611
Dumke M., Krause M., 1998, in Breitschwerdt D., Freyberg M., eds, Proc. IAU Colloq. 166, The Local Bubble and Beyond. Springer, Berlin, in press
Dumke M., Krause M., Wielebinski R., Klein U., 1995, A&A, 302, 691
Ehle M., Beck R., 1993, A&A, 273, 45
Eilek J. A., 1989a, AJ, 98, 244
Eilek J. A., 1989b, AJ, 98, 256
Elstner D., Meinel R., Beck R., 1992, A&AS, 94, 587
Gardner F. F., Whiteoak J. B., 1966, ARA&A, 4, 245
Horellou C., Beck R., Berkhuijsen E. M., Krause M., Klein U., 1992, A&A, 265, 417
Hummel E., Dahlem M., van der Hulst J. M., Sukumar S., 1991, A&A, 246, 10
Johnson R. A., Leahy J. P., Garrington S. T., 1995, MNRAS, 273, 877
Korchak A. A., Syrovatskii S. I., 1962, SvA, 5, 678
Krasheninnikova Y., Ruzmaikin A., Sokoloff D., Shukurov A., 1989, A&A, 213, 19
Laing R. A., 1981, ApJ, 248, 87
Lazio T. J., Spangler S. R., Cordes J. M., 1990, ApJ, 363, 515
Leahy J. P., 1987, MNRAS, 226, 433

Minter A. H., Spangler S. R., 1996, ApJ, 458, 194
Ohno H., Shibata S., 1993, MNRAS, 262, 953
Pacholczyk A. G., 1977, Radio Galaxies. Pergamon Press, Oxford
Panesar J. S., Nelson A. H., 1992, A&A, 264, 77
Poezd A., Shukurov A., Sokoloff D., 1993, MNRAS, 264, 285
Razin V. A., Khroulyov V. V., 1965, Soviet Izvestia Vyzov, Radiofizika 8, 1063
Ruzmaikin A. A., Shukurov A. M., Sokoloff D. D., 1988, Magnetic Fields of Galaxies. Kluwer, Dordrecht
Sokoloff D., Shukurov A., 1990, Nat, 347, 51
Spangler S. R., 1982, ApJ, 261, 310
Spangler S. R., 1983, ApJ, 271, L49
Spitzer L., 1942, ApJ, 95, 329
Sukumar S., Allen R. J., 1991, ApJ, 382, 100
Taylor G. B., Perley R. A., Inoue M., Kato T., Tabara H., Aizu K., 1990, ApJ, 360, 41
Taylor G. B., Barton E. J., Ge J., 1994, AJ, 107, 1942
Tribble P. C., 1991, MNRAS, 250, 726
Urbanik M., Elstner D., Beck R., 1997, A&A, 326, 465
Wieringa M. H., de Bruyn A. G., Jansen D., Brouw W. N., Katgert P., 1993, A&A, 268, 215

APPENDIX A: COMPLEX POLARIZATION IN A RANDOM MEDIUM

In this section we obtain an expression for the complex polarization in a random magneto-ionic medium with allowance for internal Faraday dispersion. Under conditions specified in Section 6, using equations (13) and (29), we obtain the following expression for the complex polarization:

$$\mathcal{P} = \left(\int_{-z_b}^{z_b} \langle\varepsilon\rangle_{W\times h}\, dz\right)^{-1} \times \int_{-z_b}^{z_b} \mathcal{P}_0(z)\langle\varepsilon\rangle_{W\times h} \exp\left(2i\lambda^2 \textstyle\int_z^{z_b} M\, dz'\right) \times \left\langle \exp\left(2i\lambda^2 \textstyle\int_z^{z_b} m\, dz'\right)\right\rangle_{W\times h} dz\,, \quad \text{(A1)}$$

where M is assumed to be constant across the beam.

In the same manner as in Section 5, we express the average over the beam area in terms of the ensemble average:

$$\left\langle e^{iX}\right\rangle_{W\times h} = \left\langle e^{iX}\right\rangle + N_W^{-1/2}\sigma_{\exp(iX)}\xi\,,$$

where $X = 2\lambda^2 \int_z^{z_b} m\, dz'$ and N_W is the number of correlation cells of e^{iX} within the averaging volume.

For any statistical property of the random quantity m, its integral X is well approximated by a Gaussian random variable, and we can use the following relation applicable to the ensemble average of a Gaussian random variable:

$$\left\langle e^{iX}\right\rangle \equiv (2\pi\sigma_X^2)^{-1/2}\int_{-\infty}^{\infty} \exp\left[iX - X^2(2\sigma_X^2)^{-1}\right] dX = \exp\left(-\tfrac{1}{2}\sigma_X^2\right)\,, \quad \text{(A2)}$$

where σ_X is the standard deviation of X. As $\langle X\rangle = 0$,

$$\sigma_X^2 = \left\langle X^2\right\rangle = 4\lambda^4 \int_z^{z_b}\int_z^{z_b} \left\langle m(z')m(z'')\right\rangle dz'dz''\,.$$

The average under the integral is the two-point autocorrelation function of m. As it significantly differs from zero only for $|z' - z''| \le l_m$, where l_m is the correlation scale of m along z, we have $\int_{-\infty}^{\infty} \langle m(z')m(z'')\rangle\, d(z' - z'') \simeq \sigma_m^2 l_m$, where σ_m is the standard deviation of m. We have assumed that $z_b - z \gg l_m$, which allows us to use an infinite integration domain.

Introducing intermediate variables $\frac{1}{2}(z' + z'')$ and $z' - z''$, we obtain

$$\sigma_X^2 = 4\lambda^4 l_m \int_z^{z_b} \sigma_m^2\, dz'\,. \quad \text{(A3)}$$

This expression is valid only for $z_b - z \gg l_m$. At positions closer to the boundary of the source, $z_b - z \lesssim l_m$, we have to replace l_m by $z_b - z$ in equation (A3).

We can estimate the number of correlation cells within the beam cylinder required to have fluctuations in the complex polarization smaller than the mean value in equation (30). We obtain it for a purely random medium, $\mathcal{R} = 0$. The integral of the fluctuating part over z appearing in equation (30), $\int_{-z_b}^{z_b} N_W^{-1/2}\Xi\, dz$, has the standard deviation

$$N^{-1/2}\sigma_{\exp(iX)} = N^{-1/2}[1 - \exp(-\sigma_{RM}^2\lambda^4)]^{1/2} \approx N^{-1/2},$$

where

$$X = 2\lambda^2 \int_{-z_b}^{z_b} m\, dz'$$

and we have used the relation

$$\sigma_{\exp(iX)}^2 = \left\langle e^{iX}e^{-iX}\right\rangle - \left\langle e^{iX}\right\rangle^2 = 1 - \exp\left(-\tfrac{1}{2}\sigma_X^2\right).$$

Thus,

$$\sigma_\Xi \approx 1 \text{ for } \sigma_{RM}^2\lambda^4 \gtrsim 1.$$

The average contribution is about $(2\lambda^4\sigma_{RM}^2)^{-1}$ for large λ. This yields the following constraint on the number of correlation cells within the beam cylinder:

$$N \gtrsim 4\sigma_{RM}^4\lambda^8\,,$$

which can be used to obtain a wavelength below which observations will give a predictable result. (It was assumed that the correlation scales of $\exp 2i\lambda^2 \int_z^{z_b} m dz'$ and ε are equal to each other.) For the 'standard' set of parameters used above for galactic discs, this constraint is rather loose, $N \gtrsim 10$ at $\lambda = 20$ cm. It should also be required that $N \gtrsim \sigma_\varepsilon^2/\langle\varepsilon\rangle^2$ in order to avoid strong fluctuations in the denominator of equation (A1); also this restriction is not very demanding.

APPENDIX B: FARADAY ROTATION IN A RANDOM EXTERNAL SCREEN

Specific properties of a Faraday screen are related to the fact that the volume integral in equation (13) is taken over the synchrotron source where $\langle\varepsilon\rangle_{W\times h} \neq 0$, whereas integration over z' in the exponent extends over the region occupied by the magneto-ionic material. Thus here we consider the case in which the synchrotron source has the boundary at $z = z_\varepsilon$ along the line of sight and the thermal plasma has a boundary at $z = z_b$ with $z_b > z_\varepsilon$. Then equation (13) reduces to

$$\mathcal{P} = \mathcal{P}_{int}\mathcal{P}_{ex}\,, \quad \text{(B1)}$$

$$\mathcal{P}_{ex} = \left\langle \exp 2iK\lambda^2 \textstyle\int_{z_\varepsilon}^{z_b} nB_z\, dz'\right\rangle_W\,, \quad \text{(B2)}$$

where $\mathcal{P}_{int}$ denotes the complex polarization associated with effects within the synchrotron source, which were our subject in Sections 4–6, and $\mathcal{P}_{ex}$ is due to the Faraday screen; $\langle\ldots\rangle_W$ denotes the average over the beam area. As follows from equation (B1), the effects of a Faraday screen can be considered separately from polarization within the source. The internal complex polarization $\mathcal{P}_{int}$ is still determined by equation (13), but now with z_b replaced by z_ε; this does not affect the formulae for $\mathcal{P}_{int}$ given above, as we assumed that either $z_b = z_\varepsilon$ or $z_b \to \infty$ and $z_\varepsilon \to \infty$.

As above, we represent the average over the telescope beam W in equation (B2) in terms of the ensemble average and fluctuations as

$$\mathcal{P}_{\rm ex} = \left\langle \exp 2{\rm i}K\lambda^2 \int_{z_\varepsilon}^{z_{\rm b}} nB_z \, {\rm d}z' \right\rangle + \delta\mathcal{P}_{\rm ex} \, ,$$

where $\delta\mathcal{P}_{\rm ex}$ is a complex random quantity with zero mean value. Burn (1966) calculated the above ensemble average for a Gaussian random field nB_z using equation (5) to show that

$$\left\langle \mathcal{P}_{\rm ex} \right\rangle = \exp\left(-2\sigma_{\rm RM}^2\lambda^4 + 2{\rm i}\lambda^2 \int_{z_\varepsilon}^{z_{\rm b}} M \, {\rm d}z'\right) ; \qquad \text{(B3)}$$

this expression can be obtained from equation (30) by assuming that $z_\varepsilon < z_{\rm b}$. As the regular term containing M contributes only to the imaginary part of $\left\langle \mathcal{P}_{\rm ex} \right\rangle$, a regular foreground Faraday screen produces rotation with ${\rm RM} = \mathcal{R} = \int_{z_\varepsilon}^{z_{\rm b}} M \, {\rm d}z$ without depolarization.

When $2\sigma_{\rm RM}^2\lambda^4 \gg 1$ we have $|\left\langle \mathcal{P}_{\rm ex} \right\rangle| \ll 1$, so that the polarization vectors in the (Q, U) plane are almost uniformly distributed over a circle the centre of which is at a small distance $|\left\langle \mathcal{P}_{\rm ex} \right\rangle|$ from the origin. The radius of this circle is $\sigma_{|\mathcal{P}_{\rm ex}|}$. Neglecting $|\left\langle \mathcal{P}_{\rm ex} \right\rangle|$, the fluctuations of $\mathcal{P}_{\rm ex}$ can be estimated as

$$\delta\mathcal{P}_{\rm ex} = \sigma_{|\mathcal{P}_{\rm ex}|} N_W^{-1/2} \xi \quad \text{for} \quad 2\sigma_{\rm RM}^2\lambda^4 \gg 1 \, , \qquad \text{(B4)}$$

where $\sigma_{|\mathcal{P}_{\rm ex}|}$ is the standard deviation of $|\mathcal{P}_{\rm ex}|$, $N_W = (D/2l_{\rm RM})^2$ is the number of correlation cells of RM within the telescope beam, and ξ is a complex random variable with unit modulus. Tribble (1991) showed that the correlation scale of $\mathcal{P}_{\rm ex}$ differs from that of RM and is given by

$$l_{\mathcal{P}} \simeq l_{\rm RM}(2\sigma_{\rm RM}\lambda^2)^{-1/2} \quad \text{for} \quad 2\sigma_{\rm RM}\lambda^2 \gg 1 \, , \qquad \text{(B5)}$$

where $l_{\rm RM}$ is the correlation scale of RM across the beam. Thus the area filling factor of the cells of $\mathcal{P}_{\rm ex}$, defined as $f_{\mathcal{P}} = (l_{\mathcal{P}}/l_{\rm RM})^2$, decreases as λ^{-2} and becomes small at large λ. Polarized emission with $|\mathcal{P}| \approx |\mathcal{P}_{\rm int}|$ comes from an area $l_{\mathcal{P}}^2$ in each cell of total area $l_{\rm RM}^2$; only unpolarized emission comes from the remaining part of each cell. The standard deviation of $|\mathcal{P}_{\rm ex}|$ is then given by a typical degree of polarization (normalized by $|\mathcal{P}_{\rm int}|$) coming from a single cell of RM i. e.

$$\sigma_{|\mathcal{P}_{\rm ex}|} = f_{\mathcal{P}} \simeq \frac{1}{2\sigma_{\rm RM}\lambda^2} \quad \text{for} \quad 2\sigma_{\rm RM}\lambda^2 \gg 1 \, . \qquad \text{(B6)}$$

The physical meaning of this result is that the standard deviations of the observed Stokes parameters Q and U are given by $\sigma_{Q,U} \simeq 2^{-1/2}\sigma_{|\mathcal{P}_{\rm ex}|} N_W^{-1/2}$. This estimate, together with equation (B4), applies only to the case $2\sigma_{\rm RM}\lambda^2 \gg 1$ when $\left\langle \mathcal{P}_{\rm ex} \right\rangle$ is negligible. Only then can $|\delta\mathcal{P}_{\rm ex}|$ be identified with fluctuations of the degree of polarization, $\delta p_{\rm ex}$. For $2\sigma_{\rm RM}\lambda^2 \ll 1$, fluctuations of $\mathcal{P}_{\rm ex}$ are negligible in comparison with $\left\langle \mathcal{P}_{\rm ex} \right\rangle$. In this case the distribution of the fluctuations of $\mathcal{P}_{\rm ex}$ on the complex plane (Q, U) is anisotropic, and it must be characterized by a correlation matrix rather than by a dispersion.

This paper has been typeset from a TEX/LATEX file prepared by the author.